Valorization of lipid-rich wastewaters: a theoretical analysis to tackle the competition between polyhydroxyalkanoate and triacylglyceride-storing populations

Lucía Argiz [a]*, David Correa-Galeote [b], Ángeles Val del Río [a], Anuska Mosquera-Corral [a], Rebeca González-Cabaleiro [c]

[a] CRETUS Institute, Department of Chemical Engineering, Universidade de Santiago de Compostela, 15782 Santiago de Compostela, Galicia, Spain

[b] Department of Microbiology and Institute of Water Research, Universidad de Granada, Granada, Spain

[c] Department of Biotechnology, Delft University of Technology, Van der Maasweg 9, 2629 HZ Delft, The Netherlands

* Corresponding author: luciaargiz.montes@usc.es

Highlights

- Operational conditions select for preferent TAG or PHA storage from waste lipids.
- Coupled C and N supply promotes TAG production.
- Uncoupled C and N feedings along with limited C excess favours PHA over TAG storage.
- Pathways analysis unravelled the experimentally slower synthesis of PHA than TAG.

Lab-scale operation

Enrichment SBR

Waste lipids

PHA

TAG

PHA + TAG

Feeding strategy

N availability

pH

C influx

O_2 influx

Feast and famine length

Obtainment of different products depending on the operational conditions

Need for a better understanding of the process prior its full-scale implementation

Comprehensive metabolic analysis

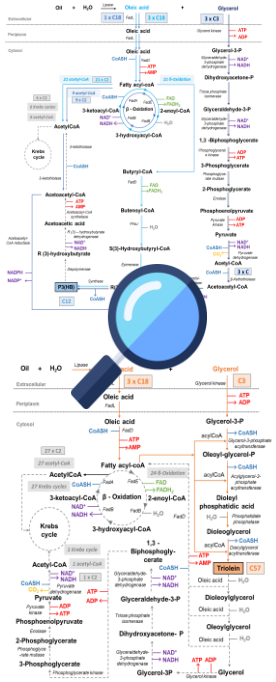

Specific operational guidelines to outcompete faster growers and select between PHA and TAG-storing populations

Coupled C & N feedings → TAG

Uncoupled C & N feedings → TAG or PHA

Function of:

- Rate of C supply
- Rate of aeration
- Feast and famine phases length

C (carbon), N (nitrogen), PHA (polyhydroxyalkanoates), SBR (sequencing batch reactor), TAG (triacylglycerides)

Valorization of lipid-rich wastewaters: a theoretical analysis to tackle the competition between polyhydroxyalkanoate and triacylglyceride-storing populations

Lucía Argiz [a] *, David Correa-Galeote [b], Ángeles Val del Río [a], Anuska Mosquera-Corral [a], Rebeca González-Cabaleiro [c]

[a] CRETUS Institute, Department of Chemical Engineering, Universidade de Santiago de Compostela, 15782 Santiago de Compostela, Galicia, Spain

[b] Department of Microbiology and Institute of Water Research, Universidad de Granada, Granada, Spain

[c] Department of Biotechnology, Delft University of Technology, Van der Maasweg 9, 2629 HZ Delft, The Netherlands

* Corresponding author: luciaargiz.montes@usc.es

ABSTRACT

The lipid fraction of the effluents generated in several food-processing activities can be transformed into polyhydroxyalkanoates (PHAs) and triacylglycerides (TAGs), through open culture biotechnologies. Although competition between storing and non-storing populations in mixed microbial cultures (MMCs) has been widely studied, the right selective environment allowing for the robust enrichment of a community when different types of accumulators coexist is still not clear. In this research, comprehensive metabolic analyses of PHA and TAG synthesis and degradation, and concomitant respiration of external carbon, were used to understand and explain the changes observed in a laboratory-scale bioreactor fed with the lipid-rich fraction (mainly oleic acid) of a wastewater stream produced in the fish-canning industry. It was concluded that the mode of oxygen, carbon, and nitrogen supply determines the enrichment of the culture in specific populations, and hence the type of intracellular compounds preferentially accumulated. Coupled carbon and nitrogen feeding regime mainly selects for TAG producers whereas uncoupled feeding leads to PHA or TAG production function of the rate of carbon supply under specific aeration rates and feast and famine phases lengths.

Keywords

Lipids; Metabolism; Microbial competition; Mixed Microbial Culture (MMC); Polyhydroxyalkanoates (PHA); Triacylglycerides (TAG)

1. INTRODUCTION

Food industries are global generators of large volumes of solid and liquid wastes. According to the Food and Agriculture Organization of the United Nations (FAO), one-third of the global food (about 130 million tonnes) is wasted adversely affecting the natural environment. Besides, conventional handling and treating methods (mainly composting, incineration, and landfilling) involve the generation of air pollutants and/or are energy-intensive and expensive further slowing down sustainable development (Jin et al., 2021; Kumar et al., 2021). In particular, fish-canneries are characterized by producing high strength liquid effluents rich in fat, oil, and grease (FOG) (Cristóvaõ et al., 2015; Monteiro et al., 2018), with concentrations that can reach up to 5 g FOG/L (Klaucans and Sams, 2018; Mannacharaju et al., 2020). These streams present fundamental operational challenges first at their collection and transportation (as they cause blockages in the sewer system), and later at their treatment (affecting oxygen transference) (Frkova et al., 2020; Wallace et al., 2017). For this reason, FOG is normally separated at a pre-treatment stage in the wastewater treatment plant (WWTP) employing different techniques (i.e. dissolved air flotation units, skimming tanks, grease traps, etc.), concomitantly generating a secondary high-loaded and complex waste stream that has to be properly managed (Klaucans and Sams, 2018). Towards the advancement of the circular economy, this stream can be valorized rather than considered an undesirable residue (Dahiya et al., 2018; Wallace et al., 2017).

Lipids can be hydrolyzed by microbial activity producing mainly free fatty acids and glycerol (Becker, 2010), which are excellent substrates for the biological cytoplasmatic storage of carbon in the form of two different intracellular compounds, polyhydroxyalkanoates (PHAs) and triacylglycerides (TAGs) (Morya et al., 2018; Patel and Matsakas, 2019; Sangkharak et al., 2020). PHAs are biodegradable polymeric molecules with great interest due to their potential to replace conventional petroleum-based plastics (Sabapathy et al., 2020). On the other hand, TAGs recovered by certain oleaginous microorganisms from waste lipids present a fatty acid profile suitable for biodiesel production (Sawangkeaw and Ngamprasertsith, 2013;

Tamis et al., 2015). Traditionally, the microbial valorization of lipid-rich streams involved expensive methods focused on the use of pure strains with a very high accumulation capacity and edible plant oils as a substrate leading to the obtainment of uncompetitive biofuels and biomaterials (Basnett et al., 2018; Pérez-Arauz et al., 2019). This fact motivated the use of residual lipid-rich streams for the production of both TAGs (Herrero et al., 2018; Lopes et al., 2018) and mostly PHAs (Mohapatra et al., 2017; Pernicova et al., 2019; Surendran et al., 2020), but it was not enough to render their production more economically feasible. To increase competitiveness, the use of waste substrates must be combined with mixed culture biotechnology and engineering designs with reduced costs and easily maintained operational conditions (Gujjala et al., 2019; Kourmentza et al., 2017; Kumar et al., 2020; Yadav et al., 2020). This solution considers engineering the ecosystem rather than specific strains to maintain a characteristic or functionality in the culture (Kourmentza et al., 2017; Mooij et al., 2013). Mooij et al. (2013) showed how to obtain a stable, open system enriched in storing populations inspired by Darwin's Theory of evolution by natural selection. To design better biotechnologies, they proposed that imposing the right selective environment can emphasize the ecological role of storage compounds, allowing for the robust enrichment of a complex culture with optimal storage capacity. However, what about competition between individuals in the community that store different intracellular compounds, and how could we target them by applying ecological selection principles? Although both PHAs and TAGs are valuable, potential applications of their mixture have not been identified, and downstream extraction and purification towards the separation of both compounds would probably have an important incidence in the process costs, reducing its competitiveness. Therefore, identification of the right selective pressures that maximize the accumulation of one storage compound and minimize the other, is fundamental towards increasing the value of the product recovered.

In this research work, we analyze the experimental shifts observed in the dominance between PHA and TAG storing populations in a 4-L enrichment sequencing batch reactor (SBR) fed with waste residual oil from the cooking water of the industrial production of canned tuna

removed in the primary treatment of the factory WWTP (Argiz et al., 2021). It was the first time that the fed of a non-pretreated oily waste stream to an open mixed microbial culture (MMC) was explored and different types of storage compounds (PHAs and TAGs) were accumulated. However, although the experimental results obtained gave some light on lipid-rich waste streams valorization and certain operational conditions seemed advantageous for one or another type of accumulators (Argiz et al., 2021), there is still an important lack of understanding concerning culture and hence product selection that limits the further development of the biotechnology.

The objective of this research was to better understand the process towards a future larger-scale implementation. For that purpose, comprehensive metabolic descriptions supported by experimental observations were used to define specific operational guidelines towards imposing suitable selective pressures for not only outcompete faster-growers but select between storing populations.

2. MATERIALS AND METHODS

2.1 Experimental procedure

A 4-L SBR was fed with waste fish oil rich in oleic acid (Table S1 of Supplementary Material (SM)). It was inoculated with activated sludge from an urban WWTP. The SBR was aerobically operated in 12 hours cycles selecting strains with high storage ability. The enrichment was carried under aerobic dynamic feeding (ADF) selection strategy, which relies on subsequent feast/famine (F/F) cycles in which the MMC is initially subjected to an excess of carbon source (feast) and then submitted to carbon deficiency (famine) (Kourmentza et al., 2017). At the end of each cycle, the reactor exchanged half of its volume (see dilution water composition in Table S2 of SM) resulting in hydraulic (HRT) and solid (SRT) retention times of 24 h.

Three operational periods were considered: I) simultaneous C (carbon) and N (nitrogen) (excess, about 1.2 g NH_4Cl/cycle) addition at the beginning of the cycle (conventional ADF,

single growth limitation strategy); II) C supply at the beginning of the cycle and N addition (limited, about 0.6 g NH_4Cl/cycle) after three hours to avoid its availability during the feast phase and restrict the growth of non-storing microorganisms (double growth limitation strategy (DGL)) (Kourmentza et al., 2017; Lorini et al., 2020); period III) same conditions as period II but feeding the N source after two hours. The amount of carbon added to the system, expressed as chemical oxygen demand concentration (COD), was 4.48 g COD/cycle in the three operational periods studied.

More details concerning the SBR configuration and operation can be found in Argiz et al. (2021), and information regarding analytical methods and calculations is summarized in Table S3 of SM.

2.2 Metabolic analysis

The pathways for oleic acid and glycerol metabolic activities were constructed supported by literature assuming oleic acid as the only fatty acid present in the substrate (see Table S1).

Biotransformation of oleic acid was considered as: synthesis and degradation of P3(HB), assuming that a unit of PHA biopolymer comprised three hydroxybutyrate (HB) units (Figure 1); triolein synthesis and degradation, describing a unit of TAG as three oleic acid units and one molecule of glycerol (Figure 2); and its direct respiration (Figure 3).

For the three catabolic pathways considered (Figures 1, 2, and 3), the number of reactions involved, the maximum ATP produced, and the oxygen required was calculated. Also, the bioenergetics of specific reactions of interest called ‘branching points’, where bifurcation between two pathways occurs, were analyzed. It is to note that P3(HB) synthesis from acetyl-CoA is not thermodynamically favorable in comparison with acetyl-CoA oxidation in the TCA cycle (Figure 1). Therefore, it was assumed that all P3(HB) synthesized from oleic acid occurred via hydroxyacyl-CoA.

The net yield of ATP was calculated as a combination of the ATP produced via substrate-level phosphorylation and the ATP yielded as a consequence of NADH (2.5 mol ATP/mol NADH)

or $FADH_2$ (1.5 mol ATP/mol $FADH_2$) oxidized per mole of substrate consumed (Shestov et al., 2013). To determine the amount of oxygen reduced to water per substrate consumed, the moles of NADH and $FADH_2$ reduced along the pathway were calculated knowing that these reduced forms release two electrons to the electron transport chain eventually consuming 0.25 moles of O_2 per electron. To have comparable data, all results were expressed per mole of carbon (Cmol).

Details regarding pathways analyses are described in SM section *"2 Metabolic pathways analysis"* and calculations are exemplified in the xlsx file "*Oleic acid metabolism calculations"*.

2.3. Microbial analysis

DNA from biomass samples was isolated using the FastDNA-2 mL SPIN Kit for Soil and the FastPrep24 apparatus (MP-BIO, USA). Two independent biological replicates were used from each sampling time.

Bacterial and fungal Illumina sequencing was made using the primers Pro341F/Pro805R (Takahashi et al., 2014) and QuantF/FungiQuantR, respectively. The pipeline analysis was performed following MothurMiSeq guidelines in the software Mothur v1.44.1 (Schlosset al. 2009). The resulting operational taxonomic units (OTUs) (97% similarity threshold and abundances higher than six sequences (relative abundance (RA) > 0.001%)) were taxonomically classified through the blast suite of the Geneious 2021.1.1 software (Biomatters, New Zealand) against the bacterial 16S rRNA and fungal 18S rRNA NCBI database (www.ftp.ncbi.nlm.nih.gov/blast/db/). Bacterial sequences were deposited in GeneBank (accession number SUB9840624). The fungal ones were retrieved from the previous dataset published by Correa-Galeote (2021b, accession number SUB9070410).

3. RESULTS AND DISCUSSION

3.1 Selection of storing compounds and microbial populations correlates with changes in operational parameters

Figure 4 shows the evolution of the main parameters controlling the process (pH, dissolved oxygen concentration (DO), PHA and TAG storage, COD, and total nitrogen (TN)) during three representative SBR enrichment cycles (all at stationary state after more than 50 cycles) of the three periods defined. As it can be observed, the dominance of TAG or PHA as storing compound correlates with specific changes in the operational parameters maintained during operation. When C and N sources were added together at the beginning of the cycle, and the N source was fed in excess (period I), only TAG storage was observed (Figure 4.A). After shifting the feeding strategy in period II (Figure 4.B) (C and N supply is uncoupled maintaining the same organic load of period II but limiting N availability), PHAs were preferentially accumulated. In period III, nitrogen source supply was brought forward one hour maintaining the rest of the operational parameters. This shifted the type of dominant storage compound obtained from PHA to TAG and allowed for the obtainment of higher intracellular storages in comparison to period I (Figure 4.C).

The operational changes made not only led to a change in product yielding but also important variations in the composition of the dominant fungal and bacterial genera present within the community. Between periods I and II fungal genus *Geotrichum* (OtuF0003) and *Mortierella* (OtuF0004) decreased their relative abundances (RAs) from 26.0 % and 22.8 %, to 6.21 % and 0.33 % respectively, whereas *Apiotrichum* (OtuF0001) increased its RA from 37.8 % to 87.2 % (Figure 5.A). This correlates with the lower degree of hydrolysis observed and the decrease in TAG storage between periods I and II (Figure 4.A, 4.B). *Geotrichum* (OtuF0003) has been reported to be cultivated on hydrophobic substrates being capable of secreting extracellular lipases (Hlavsová et al., 2009) and assimilating carbon sources such as fats and oils to use them for growth and storage (Papanikolaou et al., 2017; Patel et al., 2019). The same occurs with *Mortierella* (OtuF0004), also reported being able to secrete lipases

(Jermsuntiea et al., 2011; Kotogán et al., 2018) and produce lipids from hydrophobic substrates such as triolein or sesame oil (Papanikolaou and Aggelis, 2019). However, *Apiotrichum* (OtuF001) has been only identified as capable of growing and storing lipids on hydrophilic substrates (Papanikolaou and Aggelis, 2011a; Park et al., 1990; Qian et al., 2021; Ykema et al., 1989) and it has not been reported as a lipase producer.

For the bacterial community, *Chryseobacterium* (OtuB0003, OtuB0005) (38.5 %), *Acidovorax* (OtuB0008) (12.2 %) and *Acinetobacter* (OtuB0009) (9.0 %) were the main bacterial genera during period I (Figure 5.B). However, after changing the feeding strategy between periods I and II, genera *Chryseobacterium* (OtuB0003, OtuB0005) reduced its abundance from 38.5 % to 17.2 %, and *Acidovorax* (OtuB0008) virtually disappeared (RA < 1 %). Nonetheless, *Acinetobacter* (OtuB0007, OtuB0009, OtuB0010) raised its RA from 9.0 % to 21.2 %, and genera *Azospirillum* (OtuB0001), *Pandoraea* (OtuB0006), and *Klebsiella* (OtuB0014) went from being minority OTUs to present RAs of 21.06 %, 13.0 %, and 8.2 %, respectively (Figure 5.B). Those genera that notably raised their RAs after changing the feeding strategy were all identified as PHA storing populations, which correlated with the higher PHA storage capacity observed in period II (Figure 4.B). Bacteria belonging to genera *Azospirillum* have been reported as capable of storing high amounts of PHA from substrates like acetate, pyruvate, lactate, and malate (Alves et al., 2017; Itzigsohn et al., 1995; Martínez-Martínez et al., 2019). Regarding *Pandoraea,* it was observed to accumulate PHA from waste frying oil and other industrial by-products (de Paula et al., 2017; Kumar et al., 2017, 2018; Liu et al., 2019). Also, *Klebsiella* has been widely identified as a very promising PHA producer (Ferreira et al., 2016; Wong et al., 2002) due to the high production yields that can be obtained on low-cost substrates (Valdez-Calderón et al., 2020; Wong et al., 2002). Besides, *Klebsiella* species present an active lipase system that makes them capable to hydrolyze and assimilate hydrophobic substrates such as waste frying oil (Tufail et al., 2017). Regarding *Acinetobacter*, several research works reported the high PHA synthetic yield from a wide variety of substrates (VFAs, glucose, glycerol, etc.) including cooking oils (Giraldo-Montoya et al., 2020; Li et al.,

2020; Muangwong et al., 2016; Sabapathy et al., 2020) due to their ability to secrete lipolytic enzymes (Liu et al., 2013; Sharma et al., 2019). Nonetheless, *Acinetobacter* species are also capable of storing TAG from both hydrophilic (Alvarez and Steinbüchel, 2003; Manilla-Pérez et al., 2010; Salcedo-Vite et al., 2019; Wältermann et al., 2005) and hydrophobic substrates including olive oil (Alvarez et al., 1997; Alvarez and Steinbüchel, 2003), which explains their presence when TAGs were preferentially stored.

Between periods II and III, the fungal population shifted as *Apiotrichum's* (OtuF0001) RA decreased from 88.2 % to 2.1 %, and *Candida* (OtuF0002) (66.4 %), followed by *Fonsecaea* (OtuF0005) (18.7 %) and *Capronia* (6.9 %) were then the dominant fungal populations (Figure 5.A). This community shift correlates with the observed increase in the degree of substrate hydrolysis and TAG concentration (from PHA to TAG between periods II and III, Figure 4.B and 4.C respectively). Thus, oleaginous yeasts belonging to the genus *Candida* (OtuF0002) have been widely recorded to use not only hydrophilic but also hydrophobic substrates (i.e. triolein, olive oil, linseed oil) via the *ex novo* pathway (Dias et al., 2021; Papanikolaou and Aggelis, 2011b) and stand out by their ability to hydrolyze lipids (Theerachat et al., 2017). *Fonsecaea* (OtuF0005) has not been identified as an oleaginous fungus although it was demonstrated its ability to produce high levels of secretory lipases (Okeke and Gugnani, 1989). Besides, certain species belonging to genera *Capronia* (OTUF0007) were identified as capable of degrading lipids and exhibiting a strong lipase activity although there is no information concerning lipids storage (Untereiner and Malloch, 1999). For the bacterial community between periods II and III, *Azospirillum* (Otu0001) abundance was almost maintained (21.1 % versus 25.3 %) but PHA-storing genera *Pandoraea* (OtuB0006), *Chryseobacterium* (OtuB0003, OtuB0005), and *Klebsiella* (OtuB0014) became minority OTUs (RAs < 0.5 %). More details of the microbial community composition can be found in SM section *"3. Microbial analysis"*.

3.2 Uncoupling C and N supply shifts preferential product stored: from TAG to PHA synthesis

Simultaneous carbon and nitrogen supply (period I) does not limit microbial growth in the feast phase (Silva et al., 2017). Under these conditions, O_2 consumption for ATP production supporting growth is expected to be preferential as long as carbon is available in the reaction medium (N is supplied in excess in period I).

Selection between P3(HB) synthesis from oleic acid or its oxidation is a function of the metabolic state of the cell (Ren et al., 2009), and only high [NADH]/[NAD^+] ratios, expected under limiting O_2 conditions (De Graef et al., 1999; Sun et al., 2012), will inhibit β-Oxidation favouring S(3)-Hydroxybutyryl-CoA conversion into R(3)Hydroxybutyryl-CoA to be further polymerized into P3(HB) (see details in SM section *"2. Metabolic pathways analysis"*). For P3(HB) synthesis, out of the 18 moles of carbon in one mole of oleic acid, 14 are oxidized meanwhile 4 moles are stored in P3(HB) form (Figure 1). In presence of nitrogen excess, only if O_2 is limiting it will be more advantageous to synthesize P3(HB) from oleic acid than to oxidize it.

Overall, TAG accumulation from hydrophobic carbon sources follows the *ex novo* metabolic pathway, a growth-associated process in which intracellular lipids accumulation and respiration occur simultaneously when the carbon source is added in excess (Athenaki et al., 2018; Vasiliadou et al., 2018). Therefore, under coupled C and N feedings in excess, with no limiting O_2 conditions, COD oxidation is directed towards ATP production for growth and activation of TAG accumulation via *ex novo* pathway. This accumulation, although not preferential (maximum TAG concentrations in period I are low, 13.7 wt %), might help yeasts survive under the famine conditions. However, external COD is not fully depleted at any point of the cycle (Figure 4.A), therefore the bacterial community (Figure 5.B) can survive only through total carbon oxidation. PHA accumulation is not observed (Figure 4.A) as carbon use for growth is not nitrogen or oxygen limiting, and therefore internal [NADH]/[NAD^+] ratios are not expected to be high not enabling P3(HB) synthesis.

The uncoupling of carbon and nitrogen supply (starting period II) resulted in the observation of a shifted steady-state with the dominance of PHA storage over TAG. The feast phase without nitrogen feeding limits growth (Silva et al., 2017), which diminishes the ATP requirements of the cell. This implies that pressure towards carbon oxidation for ATP production is reduced and, under the feast famine strategy, storing populations will be pushed towards the production of storage compounds. Indeed, O_2 consumption in period II lowers in the feast phase (positive DO concentration slope, Figure 4.B), with faster COD consumption if its concentration at the end of the feast period is to be compared with the one measured in period I. This allows us to predict higher internal [NADH]/[NAD^+] ratios and therefore the unblocking of PHA production pathways.

The dominance of PHA production in the system promotes the longest O_2 consumption in the famine phase when compared with the ones observed in Figure 4.A and Figure 4.C. If in this system O_2 can be considered a proxy for ATP production, we can conclude that PHA accumulation allows longer periods of growth in the famine phase being a more successful strategy for survival in conditions of carbon starvation. The analysis of the pathways has shown us that mobilization of stored PHA is in terms of complexity, ATP production, and O_2 consumption is similar to TAG mobilization (Figure 1, Figure 2). However, previously reported observations have shown that TAG mobilization seems not to be preferential over external COD depletion but PHA consumption is (Aggelis et al., 1995; Vasiliadou et al., 2018). Thus, the LCFAs that were not consumed during the feast phase will be available as free fatty acids in the reaction medium during the famine (hydrolysis, transport, and activation were already performed in the feast phase). However, stored TAGs need to be intracellularly hydrolyzed and activated, which requires ATP (Figure 2). A similar conclusion can be drawn from our observations, as is only in period II where O_2 consumption continuous beyond external COD exhaustion (Figure 4).

3.3 Faster carbon supply shifts again the preferential product stored maintaining an uncoupled C and N feeding: from PHA to TAG synthesis

Period III starts when nitrogen feed was advanced one hour maintaining the rest of the operational parameters. The feeding of sodium bicarbonate buffer was lower in this period (see SM section *"4. pH decrease in the famine phase"*), which decreased the pH value observed at the end of each cycle (Figure 4.C). These changes seem to dramatically select for TAG accumulators (Figure 4.B versus Figure 4.C, Figure 5). TAG concentrations at the end of period III were the highest, and the culture was enriched in TAG producers (Figure 5).

Yeasts (TAG accumulators in our SBR) are well-known to possess and express an active lipase system able to hydrolize complex fatty substrates (see SM section *"3. Microbial analysis"*). The highest substrate hydrolysis was achieved in this period (it was estimated a 35% and 75% hydrolysis in periods II and III respectively, see SM section *"5. Substrate hydrolysis estimation"*), which led to a notably higher carbon bioavailability increasing the amount of metabolizable carbon in the system per unit of time (Carsanba et al., 2018). This can explain the higher biomass concentration observed once reached the steady-state operation (from 0.47 ± 0.04 g VSS/L to 0.87 ± 0.08 g VSS/L in periods II and III). Remarkably, higher biomass concentrations than in period II were achieved with similar nitrogen consumptions . This is an indicator that a significantly higher abundance of yeast versus bacterial populations was achieved: yeasts and fungi require almost half of N to produce one mole of biomass than bacteria (see SM section *"6. Nitrogen balance"*) (Milo & Phillips, 2015; Popovic, 2019).

The lower pH values reached at the end of the cycle in period III in comparison to period II (Figure 4.B, Figure 4.C) have limited the bacterial survival and enhanced the enrichment of the culture in TAG-storing microorganisms (Donot et al., 2014). Once steady-state conditions were reached, the higher carbon excess during the feast phase if compared to period II was evidenced by the evolution of COD profiles. When PHAs were preferentially stored, the carbon source was depleted before N source addition (Figure 4.B). However, in period III, extracellular

carbon was still available during the famine phase (Figure 4.C). Therefore, as in period I, systematic O_2 consumption for external carbon oxidation and growth was concomitant to TAG degradation in the famine phase. This is evidenced by the sharp decrease of dissolved oxygen after nitrogen addition (Figure 4.C). Nevertheless, under uncoupled feeding, the maximum TAG accumulation obtained was much higher than when the feeding was coupled (period I). This led to a longer period of oxygen consumption compared to the one observed in period I.

According to metabolic pathways analysis, TAG storage is a substrate-limited process in comparison with PHA. Thus, fatty acids cannot be intracellularly accumulated as reserve materials until dioleoyl phosphatidic acid dephosphorylation. Therefore, to obtain an accumulative compound (dioleoglycerol), at least two oleic acid moles and one mole of glycerol are needed (Figure 2). On the contrary, just one mole of oleic acid is needed to produce an HB unit that can be stored and further polymerized (Figure 1).

The calculated stoichiometric ratios of carbon to oxygen (see detailed calculations in SM section *"7. C/O_2 ratios for PHA and TAG synthesis"*), showed that although to favor the selection of storing populations against non-storing ones always an excess of carbon is required. As a function of the carbon excess, one or another storage compound will be preferred. Substantially higher carbon influxes promote TAG (105 mg COD/(L·h), maximum 31.8 wt % at the end of the feast phase, Figure 4.C) over PHA accumulation (33 mg COD/(L·h), maximum 32.1 wt % PHA at the end of the feast phase (Figure 4.B).

It was also observed that while PHAs were produced at a rate of 0.182 Cmol PHA/(Cmol substrate·h) reaching the maximum accumulation capacity after three hours (2.15 steps/Cmol and 2.92 steps/Cmol via hydroxyacyl-CoA and acetyl-CoA, respectively) (Figure 4.B), TAG storage rate was almost the double (0.349 Cmol TAG/(Cmol substrate·h) obtaining the maximum intracellular storage after only 1.5 hours (0.35 steps/Cmol) (Figure 4.C). PHA synthesis appears as a more complex process than triolein accumulation (Figure 1; Figure 2), which can explain why the maximum storage capacity for PHA was achieved later than for TAG (Figure 4.B versus Figure 4.C). It can also explain why under fast rates of carbon feed,

the conversion of carbon into PHA becomes rate-limiting, giving an advantage to the faster synthesis of TAGs. Triolein yielding only requires oleic acid transport and acylation in the cytoplasm of the cell (Figure 2) whereas P3(HB) production involves the transformation of oleic acid via β-oxidation cycle (Figure 1) in a pathway 1.80 steps/Cmol longer than the one required for triolein production using the same substrate.

In our experiment, the decrease of pH must play a role in the observed enrichment in yeast happening during period III. This probably enhanced hydrolysis of the substrate, allowing for higher carbon availability despite maintaining the same feed regime. The maximum TAG accumulation observed in our experiments was reached in this period. It was associated with remarkable higher hydrolysis and an earlier nitrogen feeding, which supports our hypothesis that a high carbon supply is necessary to systematically select for TAG production when C and N feeds are uncoupled.

4. CONCLUSIONS AND RECOMMENDATIONS

Long-chain fatty acids and glycerol present in lipid-rich streams serve as precursors for the microbial production of two different added-value compounds, PHAs and TAGs. Through this research, guidelines to engineering the competition between PHA and TAG-storing populations in an open community aiming for the preferent and most efficient obtainment of one or another storage compound were defined. Towards further process optimization and future large scale implementation of the biotechnology, the following outcomes should be taken into consideration:

- Avoid simultaneous oleaginous carbon and nitrogen feedings to select for PHA accumulators as it seems highly unlikely under these conditions (period I). Carbon consumption will be preferentially used for respiration and because PHA accumulation is a rate-limiting process compared with TAG synthesis, the latter will be more efficient when competing for the external carbon available. Moreover, TAG accumulation

happens simultaneously to respiration processes while PHA synthesis requires a metabolic decision between ATP production or internal carbon storage.

- To increase intracellular accumulation uncouple carbon and nitrogen sources supply. This feeding strategy promotes higher concentrations of storage compounds under similar length of famine periods. It was observed maximum intracellular accumulations (as a sum of PHA and TAG) of 38 wt % and 32 wt % in periods II and III (uncoupled), and 15 wt % in period I (coupled). Switching between preferential PHA or TAG accumulation depends on the operational conditions (period II and period III, respectively) and comes together with the measurement of higher relative abundances of PHA storing populations or oleaginous microorganisms (responsible for substrate hydrolysis and TAG storage; mainly yeast).
- Higher rates of hydrolysis and nitrogen supply in presence of external carbon, seems to favour preferential TAG production (period III). This can be explained by faster rates for TAG synthesis than for PHA (0.349 Cmol TAG/(Cmol substrate·h) vs. 0.182 Cmol PHA/(Cmol substrate·h), which correlates with the theoretical analysis that shows PHA synthesis to be a more complex process. Besides, yeasts present the capacity to concomitantly use external carbon for respiration and accumulation.
- To select PHA producers, the carbon excess has to be limited (in our experiments, low hydrolysis), and preferentially, the external substrate should be depleted before nitrogen addition (period II). This can be explained by the lower carbon to oxygen stoichiometric ratio calculated for PHA synthesis than for TAG (0.60 and 2.02, respectively).

5. ACKNOWLEDGMENTS

The authors thank the members of the TU Delft Environmental Biotechnology Section for the good scientific discussions, which notably helped us to improve the quality of this paper. This research was supported by the Spanish Government (AEI) through the TREASURE project [CTQ2017-83225-C2-1-R]. Lucía Argiz is a Xunta de Galicia fellow (2019), [ED 481A-2019/083], grant cofounded by the operative program FSE Galicia 2014-2020. Lucía Argiz, Ángeles Val del Río, and Anuska Mosquera-Corral belong to the Galician Competitive Research Group GRC ED431C 2017/29. All these programs are co-funded by the FEDER (EU).

6. REFERENCES

Aggelis, G., Komaitis, M., Papanikolaou, S., Papadopoulos, G., 1995. A mathematical model for the study of lipid accumulation in oleaginous microorganisms. I. Lipid accumulation during growth of Mucor circinelloides CBS 172-27 on a vegetable oil. Grasas y Aceites 46, 169–173. https://doi.org/10.3989/gya.1995.v46.i3.921

Alves, L.P.S., Almeida, A.T., Cruz, L.M., Pedrosa, F.O., de Souza, E.M., Chubatsu, L.S., Müller-Santos, M., Valdameri, G., 2017. A simple and efficient method for poly-3-hydroxybutyrate quantification in diazotrophic bacteria within 5 minutes using flow cytometry. Brazilian J. Med. Biol. Res. 50, 1–10. https://doi.org/10.1590/1414-431X20165492

Argiz, L., González-Cabaleiro, R., Val del Río, Á., González-López, J., Mosquera-Corral, A., 2021. A novel strategy for triacylglycerides and polyhydroxyalkanoates production using waste lipids. Sci. Total Environ. 763. https://doi.org/10.1016/j.scitotenv.2020.142944

Athenaki, M., Gardeli, C., Diamantopoulou, P., Tchakouteu, S.S., Sarris, D., Philippoussis, A., Papanikolaou, S., 2018. Lipids from yeasts and fungi: physiology, production and analytical considerations. J. Appl. Microbiol. 124, 336–367.

https://doi.org/10.1111/jam.13633

Basnett, P., Marcello, E., Lukasiewicz, B., Panchal, B., Nigmatullin, R., Knowles, J.C., Roy, I., 2018. Biosynthesis and characterization of a novel, biocompatible medium chain length polyhydroxyalkanoate by Pseudomonas mendocina CH50 using coconut oil as the carbon source. J. Mater. Sci. Mater. Med. 29. https://doi.org/10.1007/s10856-018-6183-9

Becker, P., 2010. Understanding and Optimizing the Microbial Degradation of Olive Oil: A Case Study with the Thermophilic Bacterium Geobacillus thermoleovorans IHI-91, Olives and Olive Oil in Health and Disease Prevention. Elsevier Inc. https://doi.org/10.1016/B978-0-12-374420-3.00042-5

Carsanba, E., Papanikolaou, S., Erten, H., 2018. Production of oils and fats by oleaginous microorganisms with an emphasis given to the potential of the nonconventional yeast Yarrowia lipolytica. Crit. Rev. Biotechnol. 38, 1230–1243. https://doi.org/10.1080/07388551.2018.1472065

Cristóvaõ, R.O., Botelho, C.M., Martins, R.J.E., Loureiro, J.M., Boaventura, R.A.R., 2015. Fish canning industry wastewater treatment for water reuse - A case Study. J. Clean. Prod. 87, 603–612. https://doi.org/10.1016/j.jclepro.2014.10.076

Dahiya, S., Kumar, A.N., Shanthi Sravan, J., Chatterjee, S., Sarkar, O., Mohan, S.V., 2018. Food waste biorefinery: Sustainable strategy for circular bioeconomy. Bioresour. Technol. 248, 2–12. https://doi.org/10.1016/j.biortech.2017.07.176

De Graef, M.R., Alexeeva, S., Snoep, J.L., Teixeira De Mattos, M.J., 1999. The steady-state internal redox state (NADH/NAD) reflects the external redox state and is correlated with catabolic adaptation in Escherichia coli. J. Bacteriol. 181, 2351–2357. https://doi.org/10.1128/jb.181.8.2351-2357.1999

de Paula, F.C., Kakazu, S., de Paula, C.B.C., Gomez, J.G.C., Contiero, J., 2017. Polyhydroxyalkanoate production from crude glycerol by newly isolated Pandoraea sp.

Polyhydroxyalkanoate production from crude glycerol. J. King Saud Univ. - Sci. 29, 166–173. https://doi.org/10.1016/j.jksus.2016.07.002

Dias, K.B., Oliveira, N.M.L., Brasil, B.S.A.F., Vieira-Almeida, E.C., Paula-Elias, F.C., Almeida, A.F., 2021. Simultaneous High Nutritional Single Cell Oil and Lipase Production By Candida Viswanathii. Acta Sci. Pol. Technol. Aliment. 20, 93–102. https://doi.org/10.17306/J.AFS.0856

Donot, F., Fontana, A., Baccou, J.C., Strub, C., Schorr-Galindo, S., 2014. Single cell oils (SCOs) from oleaginous yeasts and moulds: Production and genetics. Biomass and Bioenergy 68, 135–150. https://doi.org/10.1016/j.biombioe.2014.06.016

Ferreira, A.M., Queirós, D., Gagliano, M.C., Serafim, L.S., Rossetti, S., 2016. Polyhydroxyalkanoates-accumulating bacteria isolated from activated sludge acclimatized to hardwood sulphite spent liquor. Ann. Microbiol. 66, 833–842. https://doi.org/10.1007/s13213-015-1169-z

Frkova, Z., Venditti, S., Herr, P., Hansen, J., 2020. Assessment of the production of biodiesel from urban wastewater-derived lipids. Resour. Conserv. Recycl. 162, 105044. https://doi.org/10.1016/j.resconrec.2020.105044

Giraldo-Montoya, J.M., Castaño-Villa, G.J., Rivera-Páez, F.A., 2020. Bacteria from industrial waste: potential producers of polyhydroxyalkanoates (PHAs) in Manizales, Colombia. Environ. Monit. Assess. 192. https://doi.org/10.1007/s10661-020-08461-5

Gujjala, L.K.S., Kumar, S.P.J., Talukdar, B., Dash, A., Kumar, S., Sherpa, K.C., Banerjee, R., 2019. Biodiesel from oleaginous microbes: opportunities and challenges. Biofuels 10, 45–59. https://doi.org/10.1080/17597269.2017.1402587

Herrero, O.M., Villalba, M.S., Lanfranconi, M.P., Alvarez, H.M., 2018. Rhodococcus bacteria as a promising source of oils from olive mill wastes. World J. Microbiol. Biotechnol. 34, 0. https://doi.org/10.1007/s11274-018-2499-3

Hlavsová, K., Zarevúcka, M., Wimmer, Z., Macková, M., Sovová, H., 2009. Geotrichum

candidum 4013: Extracellular lipase versus cell-bound lipase from the single strain. J. Mol. Catal. B Enzym. 61, 188–193. https://doi.org/10.1016/j.molcatb.2009.06.012

Itzigsohn, R., Yarden, O., Okon, Y., 1995. Polyhydroxyalkanoate analysis in Azospirillum brasilense. Can. J. Microbiol. 41, 73–76. https://doi.org/10.1139/m95-171

Jermsuntiea, W., Aki, T., Toyoura, R., Iwashita, K., Kawamoto, S., Ono, K., 2011. Purification and characterization of intracellular lipase from the polyunsaturated fatty acid-producing fungus Mortierella alliacea. N. Biotechnol. 28, 158–164. https://doi.org/10.1016/j.nbt.2010.09.007

Jin, C., Sun, S., Yang, D., Sheng, W., Ma, Y., He, W., Li, G., 2021. Anaerobic digestion: An alternative resource treatment option for food waste in China. Sci. Total Environ. 779, 146397. https://doi.org/10.1016/j.scitotenv.2021.146397

Klaucans, E., Sams, K., 2018. Problems with fat, oil, and grease (FOG) in food industry wastewaters and recovered FOG recycling methods using anaerobic co-digestion: A short review. Key Eng. Mater. 762, 61–68. https://doi.org/10.4028/www.scientific.net/KEM.762.61

Kotogán, A., Zambrano, C., Kecskeméti, A., Varga, M., Szekeres, A., Papp, T., Vágvölgyi, C., Takó, M., 2018. An organic solvent-tolerant lipase with both hydrolytic and synthetic activities from the oleaginous fungus mortierella echinosphaera. Int. J. Mol. Sci. 19, 1–16. https://doi.org/10.3390/ijms19041129

Kourmentza, C., Plácido, J., Venetsaneas, N., Burniol-Figols, A., Varrone, C., Gavala, H.N., Reis, M.A.M., 2017. Recent Advances and Challenges towards Sustainable Polyhydroxyalkanoate (PHA) Production. Bioengineering 4, 55. https://doi.org/10.3390/bioengineering4020055

Kumar, M., Dutta, S., You, S., Luo, G., Zhang, S., Show, P.L., Sawarkar, A.D., Singh, L., Tsang, D.C.W., 2021. A critical review on biochar for enhancing biogas production from anaerobic digestion of food waste and sludge. J. Clean. Prod. 305, 127143.

https://doi.org/10.1016/j.jclepro.2021.127143

Kumar, M., Rathour, R., Singh, R., Sun, Y., Pandey, A., Gnansounou, E., Andrew Lin, K.Y., Tsang, D.C.W., Thakur, I.S., 2020. Bacterial polyhydroxyalkanoates: Opportunities, challenges, and prospects. J. Clean. Prod. 263, 121500. https://doi.org/10.1016/j.jclepro.2020.121500

Kumar, M., Singhal, A., Verma, P.K., Thakur, I.S., 2017. Production and Characterization of Polyhydroxyalkanoate from Lignin Derivatives by Pandoraea sp. ISTKB. ACS Omega 2, 9156–9163. https://doi.org/10.1021/acsomega.7b01615

Kumar, Madan, Verma, S., Gazara, R.K., Kumar, Manish, Pandey, A., Verma, P.K., Thakur, I.S., 2018. Genomic and proteomic analysis of lignin degrading and polyhydroxyalkanoate accumulating β-proteobacterium Pandoraea sp. ISTKB. Biotechnol. Biofuels 11, 1–23. https://doi.org/10.1186/s13068-018-1148-2

Li, D., Yin, F., Ma, X., 2020. Towards biodegradable polyhydroxyalkanoate production from wood waste: Using volatile fatty acids as conversion medium. Bioresour. Technol. 299, 122629. https://doi.org/10.1016/j.biortech.2019.122629

Liu, C., Wang, H., Xing, W., Wei, L., 2013. Composition diversity and nutrition conditions for accumulation of polyhydroxyalkanoate (PHA) in a bacterial community from activated sludge. Appl. Microbiol. Biotechnol. 97, 9377–9387. https://doi.org/10.1007/s00253-013-5165-6

Liu, D., Yan, X., Si, M., Deng, X., Min, X., Shi, Y., Chai, L., 2019. Bioconversion of lignin into bioplastics by Pandoraea sp. B-6: molecular mechanism. Environ. Sci. Pollut. Res. 26, 2761–2770. https://doi.org/10.1007/s11356-018-3785-1

Lopes, M., Gomes, A.S., Silva, C.M., Belo, I., 2018. Microbial lipids and added value metabolites production by Yarrowia lipolytica from pork lard. J. Biotechnol. 265, 76–85. https://doi.org/10.1016/j.jbiotec.2017.11.007

Lorini, L., di Re, F., Majone, M., Valentino, F., 2020. High rate selection of PHA accumulating

mixed cultures in sequencing batch reactors with uncoupled carbon and nitrogen feeding. N. Biotechnol. 56, 140–148. https://doi.org/10.1016/j.nbt.2020.01.006

Mannacharaju, M., Kannan Villalan, A., Shenbagam, B., Karmegam, P.M., Natarajan, P., Somasundaram, S., Arumugam, G., Ganesan, S., 2020. Towards sustainable system configuration for the treatment of fish processing wastewater using bioreactors. Environ. Sci. Pollut. Res. 27, 353–365. https://doi.org/10.1007/s11356-019-06909-x

Martínez-Martínez, M. de los A., González-Pedrajo, B., Dreyfus, G., Soto-Urzúa, L., Martínez-Morales, L.J., 2019. Phasin PhaP1 is involved in polyhydroxybutyrate granules morphology and in controlling early biopolymer accumulation in Azospirillum brasilense Sp7. AMB Express 9. https://doi.org/10.1186/s13568-019-0876-4

Mohapatra, S., Sarkar, B., Samantaray, D.P., Daware, A., Maity, S., Pattnaik, S., Bhattacharjee, S., 2017. Bioconversion of fish solid waste into PHB using Bacillus subtilis based submerged fermentation process. Environ. Technol. (United Kingdom) 38, 3201–3208. https://doi.org/10.1080/09593330.2017.1291759

Monteiro, A., Paquincha, D., Martins, F., Queirós, R.P., Saraiva, J.A., Švarc-Gajić, J., Nastić, N., Delerue-Matos, C., Carvalho, A.P., 2018. Liquid by-products from fish canning industry as sustainable sources of ω3 lipids. J. Environ. Manage. 219, 9–17. https://doi.org/10.1016/j.jenvman.2018.04.102

Mooij, P.R., Stouten, G.R., Tamis, J., Van Loosdrecht, M.C.M., Kleerebezem, R., 2013. Survival of the fattest. Energy Environ. Sci. 6, 3404–3406. https://doi.org/10.1039/c3ee42912a

Morya, R., Kumar, M., Thakur, I.S., 2018. Utilization of glycerol by Bacillus sp. ISTVK1 for production and characterization of Polyhydroxyvalerate. Bioresour. Technol. Reports 2, 1–6. https://doi.org/10.1016/j.biteb.2018.03.002

Muangwong, A., Boontip, T., Pachimsawat, J., Napathorn, S.C., 2016. Medium chain length polyhydroxyalkanoates consisting primarily of unsaturated 3-hydroxy-5-cis-dodecanoate

558 synthesized by newly isolated bacteria using crude glycerol. Microb. Cell Fact. 15, 1–17.
559 https://doi.org/10.1186/s12934-016-0454-2

560 Papanikolaou, S., Aggelis, G., 2019. Sources of microbial oils with emphasis to Mortierella
561 (Umbelopsis) isabellina fungus. World J. Microbiol. Biotechnol. 35, 1–19.
562 https://doi.org/10.1007/s11274-019-2631-z

563 Papanikolaou, S., Aggelis, G., 2011a. Review Article Lipids of oleaginous yeasts . Part I :
564 Biochemistry of single cell oil production 1031–1051.
565 https://doi.org/10.1002/ejlt.201100014

566 Papanikolaou, S., Aggelis, G., 2011b. Lipids of oleaginous yeasts. Part II: Technology and
567 potential applications. Eur. J. Lipid Sci. Technol. 113, 1052–1073.
568 https://doi.org/10.1002/ejlt.201100015

569 Papanikolaou, S., Rontou, M., Belka, A., Athenaki, M., Gardeli, C., Mallouchos, A., Kalantzi,
570 O., Koutinas, A.A., Kookos, I.K., Zeng, A.P., Aggelis, G., 2017. Conversion of biodiesel-
571 derived glycerol into biotechnological products of industrial significance by yeast and
572 fungal strains. Eng. Life Sci. 17, 262–281. https://doi.org/10.1002/elsc.201500191

573 Park, W.S., Murphy, P.A., Glatz, B.A., 1990. Lipid metabolism and cell composition of the
574 oleaginous yeast Apiotrichum curvatum grown at different carbon to nitrogen ratios. Can.
575 J. Microbiol. 36, 318–326. https://doi.org/10.1139/m90-056

576 Patel, A., Matsakas, L., 2019. A comparative study on de novo and ex novo lipid fermentation
577 by oleaginous yeast using glucose and sonicated waste cooking oil. Ultrason. Sonochem.
578 52, 364–374. https://doi.org/10.1016/j.ultsonch.2018.12.010

579 Patel, A., Pruthi, V., Pruthi, P.A., 2019. Innovative screening approach for the identification of
580 triacylglycerol accumulating oleaginous strains. Renew. Energy 135, 936–944.
581 https://doi.org/10.1016/j.renene.2018.12.078

582 Pérez-Arauz, A.O., Aguilar-Rabiela, A.E., Vargas-Torres, A., Rodríguez-Hernández, A.I.,
583 Chavarría-Hernández, N., Vergara-Porras, B., López-Cuellar, M.R., 2019. Production

584 and characterization of biodegradable films of a novel polyhydroxyalkanoate (PHA)
585 synthesized from peanut oil. Food Packag. Shelf Life 20, 100297.
586 https://doi.org/10.1016/j.fpsl.2019.01.001

587 Pernicova, I., Kucera, D., Nebesarova, J., Kalina, M., Novackova, I., Koller, M., Obruca, S.,
588 2019. Production of polyhydroxyalkanoates on waste frying oil employing selected
589 Halomonas strains. Bioresour. Technol. 292, 122028.
590 https://doi.org/10.1016/j.biortech.2019.122028

591 Popovic, M., 2019. Thermodynamic properties of microorganisms: determination and analysis
592 of enthalpy, entropy, and Gibbs free energy of biomass, cells and colonies of 32
593 microorganism species. Heliyon 5, e01950.
594 https://doi.org/10.1016/j.heliyon.2019.e01950

595 Publishers, K.A., 1989. Lipases of Fonsecaea pedrosoi and Phialophora verrucosa Lipase
596 production Lipase assay The lipase activity was estimated titrimetrically (Somkuti &
597 Babel 1968). One 324, 313–324.

598 Qian, X., Zhou, X., Chen, L., Zhang, X., Xin, F., Dong, W., Zhang, W., Ochsenreither, K.,
599 Jiang, M., 2021. Bioconversion of volatile fatty acids into lipids by the oleaginous yeast
600 Apiotrichum porosum DSM27194. Fuel 290, 119811.
601 https://doi.org/10.1016/j.fuel.2020.119811

602 Ren, Q., De Roo, G., Ruth, K., Witholt, B., Zinn, M., Thöny-Meyer, L., 2009. Simultaneous
603 accumulation and degradation of polyhydroxyalkanoates: Futile cycle or clever
604 regulation? Biomacromolecules 10, 916–922. https://doi.org/10.1021/bm801431c

605 Sabapathy, P.C., Devaraj, S., Meixner, K., Anburajan, P., Kathirvel, P., Ravikumar, Y., Zabed,
606 H.M., Qi, X., 2020. Recent developments in Polyhydroxyalkanoates (PHAs) production –
607 A review. Bioresour. Technol. 123132. https://doi.org/10.1016/j.biortech.2020.123132

608 Sangkharak, K., Paichid, N., Yunu, T., Klomklao, S., Prasertsan, P., 2020. Utilisation of tuna
609 condensate waste from the canning industry as a novel substrate for

610 polyhydroxyalkanoate production. Biomass Convers. Biorefinery.
611 https://doi.org/10.1007/s13399-019-00581-4

612 Sawangkeaw, R., Ngamprasertsith, S., 2013. A review of lipid-based biomasses as feedstocks
613 for biofuels production. Renew. Sustain. Energy Rev. 25, 97–108.
614 https://doi.org/10.1016/j.rser.2013.04.007

615 Sharma, P.K., Mohanan, N., Sidhu, R., Levin, D.B., 2019. Colonization and degradation of
616 polyhydroxyalkanoates by lipase-producing bacteria. Can. J. Microbiol. 65, 461–475.
617 https://doi.org/10.1139/cjm-2019-0042

618 Shestov, A.A., Mancuso, A., Leeper, D.B., Glickson, J.D., 2013. Metabolic network analysis
619 of DB1 melanoma cells: How much energy is derived from aerobic glycolysis? Adv. Exp.
620 Med. Biol. 765, 265–271. https://doi.org/10.1007/978-1-4614-4989-8_37

621 Silva, F., Campanari, S., Matteo, S., Valentino, F., Majone, M., Villano, M., 2017. Impact of
622 nitrogen feeding regulation on polyhydroxyalkanoates production by mixed microbial
623 cultures. N. Biotechnol. 37, 90–98. https://doi.org/10.1016/j.nbt.2016.07.013

624 Sun, F., Dai, C., Xie, J., Hu, X., 2012. Biochemical issues in estimation of cytosolic free
625 NAD/NADH ratio. PLoS One 7, 31–36. https://doi.org/10.1371/journal.pone.0034525

626 Surendran, A., Lakshmanan, M., Chee, J.Y., Sulaiman, A.M., Thuoc, D. Van, Sudesh, K.,
627 2020. Can Polyhydroxyalkanoates Be Produced Efficiently From Waste Plant and Animal
628 Oils? Front. Bioeng. Biotechnol. 8. https://doi.org/10.3389/fbioe.2020.00169

629 Takahashi, S., Tomita, J., Nishioka, K., Hisada, T., Nishijima, M., 2014. Development of a
630 prokaryotic universal primer for simultaneous analysis of Bacteria and Archaea using
631 next-generation sequencing. PLoS One 9. https://doi.org/10.1371/journal.pone.0105592

632 Tamis, J., Sorokin, D.Y., Jiang, Y., Van Loosdrecht, M.C.M., Kleerebezem, R., 2015. Lipid
633 recovery from a vegetable oil emulsion using microbial enrichment cultures. Biotechnol.
634 Biofuels 8, 1–11. https://doi.org/10.1186/s13068-015-0228-9

635 Theerachat, M., Tanapong, P., Chulalaksananukul, W., 2017. The culture or co-culture of
636 Candida rugosa and Yarrowia lipolytica strain rM-4A, or incubation with their crude
637 extracellular lipase and laccase preparations, for the biodegradation of palm oil mill
638 wastewater. Int. Biodeterior. Biodegrad. 121, 11–18.
639 https://doi.org/10.1016/j.ibiod.2017.03.002

640 Tufail, S., Munir, S., Jamil, N., 2017. Variation analysis of bacterial polyhydroxyalkanoates
641 production using saturated and unsaturated hydrocarbons. Brazilian J. Microbiol. 48,
642 629–636. https://doi.org/10.1016/j.bjm.2017.02.008

643 Untereiner, W.A., Malloch, D., 1999. Patterns of substrate utilization in species of Capronia
644 and allied black yeasts: Ecological and taxonomic implications. Mycologia 91, 417–427.
645 https://doi.org/10.2307/3761342

646 Valdez-Calderón, A., Barraza-Salas, M., Quezada-Cruz, M., Islas-Ponce, M.A., Angeles-
647 Padilla, A.F., Carrillo-Ibarra, S., Rodríguez, M., Rojas-Avelizapa, N.G., Garrido-
648 Hernández, A., Rivas-Castillo, A.M., 2020. Production of polyhydroxybutyrate (PHB) by
649 a novel Klebsiella pneumoniae strain using low-cost media from fruit peel residues.
650 Biomass Convers. Biorefinery. https://doi.org/10.1007/s13399-020-01147-5

651 Vasiliadou, I.A., Bellou, S., Daskalaki, A., Tomaszewska-Hetman, L., Chatzikotoula, C.,
652 Kompoti, B., Papanikolaou, S., Vayenas, D., Pavlou, S., Aggelis, G., 2018.
653 Biomodification of fats and oils and scenarios of adding value on renewable fatty
654 materials through microbial fermentations: Modelling and trials with Yarrowia lipolytica.
655 J. Clean. Prod. 200, 1111–1129. https://doi.org/10.1016/j.jclepro.2018.07.187

656 Wallace, T., Gibbons, D., O'Dwyer, M., Curran, T.P., 2017. International evolution of fat, oil
657 and grease (FOG) waste management – A review. J. Environ. Manage. 187, 424–435.
658 https://doi.org/10.1016/j.jenvman.2016.11.003

659 Wong, P.A.L., Chua, H., Lo, W., Lawford, H.G., Yu, P.H., 2002. Production of specific
660 copolymers of polyhydroxyalkanoates from industrial waste. Appl. Biochem. Biotechnol.

661 - Part A Enzym. Eng. Biotechnol. 98–100, 655–662. https://doi.org/10.1385/ABAB:98-
662 100:1-9:655

663 Yadav, B., Pandey, A., Kumar, L.R., Tyagi, R.D., 2020. Bioconversion of waste
664 (water)/residues to bioplastics- A circular bioeconomy approach. Bioresour. Technol.
665 298, 122584. https://doi.org/10.1016/j.biortech.2019.122584

666 Ykema, A., Kater, M.M., Smit, H., 1989. Lipid production in wheypermeate by an unsaturated
667 fatty acid mutant of the oleaginous yeast Apiotrichum curvatum. Biotechnol. Lett. 11,
668 477–482. https://doi.org/10.1007/BF01026645

669

FIGURE CAPTIONS

Figure 1. Metabolic pathways and calculations of P3(HB) synthesis from three mol of oleic acid via 3-hydroxyacyl-coA (-), from one mol of oleic acid via acetyl-CoA (-), from three mol of glycerol (-), and degradation of 1 mol of P3(HB) (--). Abbreviations: fadA (β-kethotiolase), fadB (3.hydroxyacyl-CoA dehydrogenase/enoyl-CoA hydrase), fadD (acyl-CoA synthetase), fadE (acyl-CoA dehydrogenase), fadL (long chain fatty acid transport protein), PhaJ (R)-3-enoyl-CoA hydratase. P3(HB) storage (basis: 3 mol oleic acid): 2.15 steps/Cmol, 1.58 ATP/Cmol, 0.42 mol O_2/Cmol. P3(HB) degradation (basis 1 mol P3(HB)): 5.92 steps/Cmol, 5.13 ATP/Cmol, 1.13 mol O_2/Cmol.

Figure 2. Metabolic pathways and calculations regarding triolein synthesis from three oleic acid units and one mol of glycerol (-), and its degradation (--). Abbreviations: fadA (β-kethotiolase), fadB (3-hydroxyacyl-CoA dehydrogenase/enoyl-CoA hydrase), fadD (acyl-CoA synthetase), fadE (acyl-CoA dehydrogenase), fadL (long chain fatty acid transport protein). Triolein storage (basis: 3 mol oleic acid + 1 mol glycerol): 0.35 steps/Cmol, - 0.12 ATP/Cmol, 0.00 mol O_2/Cmol. Triolein degradation (basis 1 mol triolein): 6.98 steps/Cmol, 6.64 ATP/Cmol, 1.43 mol O_2/Cmol.

Figure 3. Metabolic pathways and calculations concerning the respiration of one mol of oleic acid (-) and one mol of glycerol (-). Abbreviations: fadA (β-kethotiolase), fadB (3.hydroxyacyl-CoA dehydrogenase/enoyl-CoA hydrase), fadD (acyl-CoA synthetase), fadE (acyl-CoA dehydrogenase), fadL (long chain fatty acid transport protein). Respiration (basis: 1 mol glycerol): 7.11 steps/Cmol, 6.67 ATP/Cmol, 1.44 mol O_2/Cmol. Respiration (basis: 1 mol oleic acid): 6.33 steps/Cmol, 5.33 ATP/Cmol, 0.50 mol O_2/Cmol.

Figure 4. PHB (●), TAG (●), pH (♦) , DO (-), TN (●), and COD* (●) profiles evolution in representative SBR cycles (steady-state) during periods I (A), II (B) and III (C). *Initial COD values (1,120 g/L) are referred to the amount of non-hydrolysed oily substrate added to the system at the beginning of the cycle. These were calculated dividing the mg of COD added at the beginning of the cycle (determined from the substrate COD (mg/g), its density (g/L) and the volume fed (L)) by the bioreactor volume (L). The discontinuous vertical line represented in this figure defines the end of the feast phase and the beginning of the famine.

Figure 5. Average relative abundances of dominant (RA > 1%) A) fungal, and B) bacterial OTUs identified by high throughput Illumina sequencing in enriched activated sludge samples (n=2) during periods I – III.

Figure 1

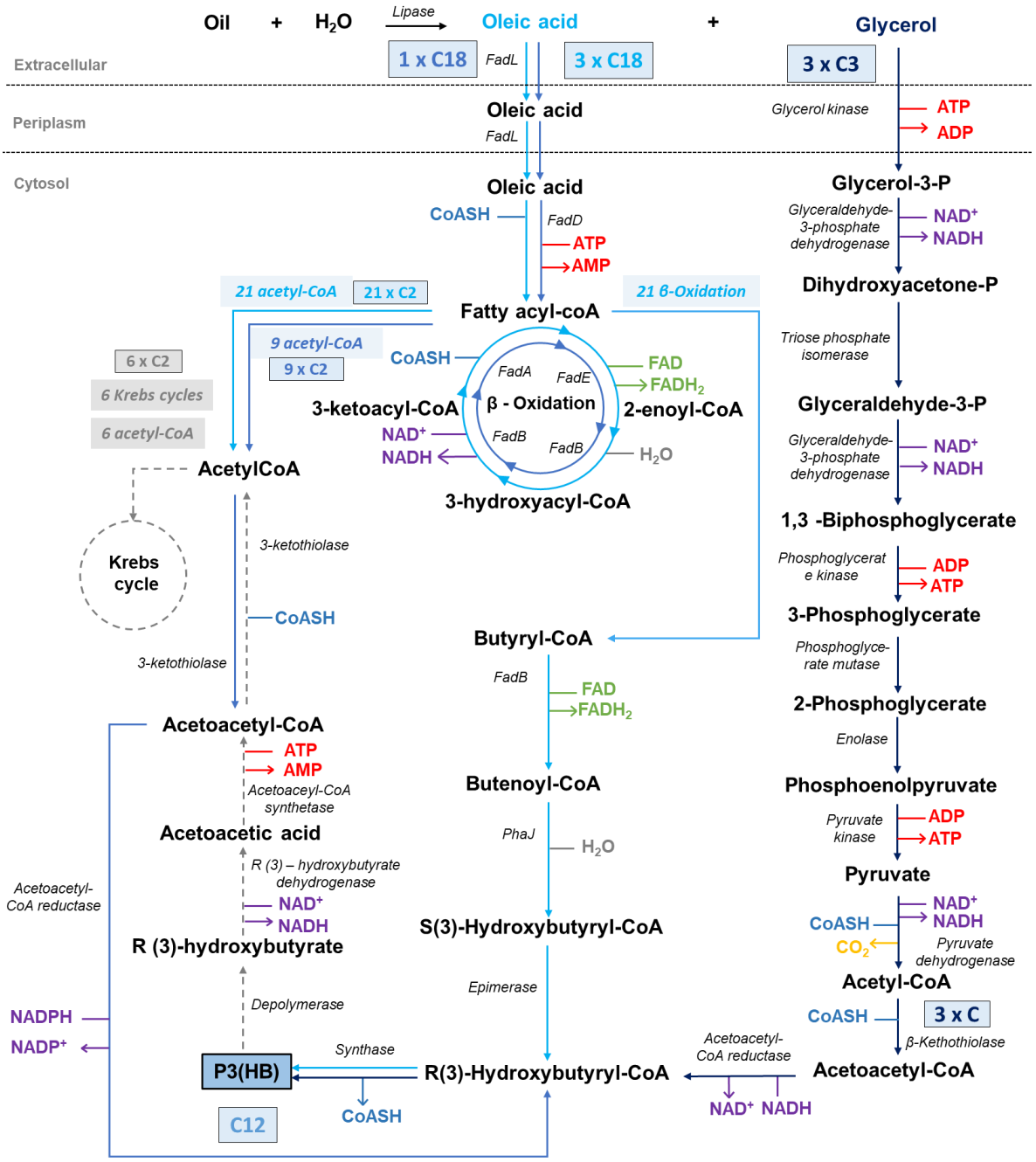
Oil + H_2O
Lipase
Oleic acid
+
Glycerol
Extracellular
1 x C18
FadL
3 x C18
3 x C3
Periplasm
Oleic acid
FadL
Glycerol kinase
ATP
ADP
Cytosol
Oleic acid
Glycerol-3-P
CoASH
FadD
ATP
AMP
Glyceraldehyde-3-phosphate dehydrogenase
NAD+
NADH
21 acetyl-CoA
21 x C2
21 β-Oxidation
Fatty acyl-coA
Dihydroxyacetone-P
9 acetyl-CoA
9 x C2
CoASH
FadA
FadE
FAD
$FADH_2$
Triose phosphate isomerase
6 x C2
6 Krebs cycles
6 acetyl-CoA
3-ketoacyl-CoA
β - Oxidation
2-enoyl-CoA
Glyceraldehyde-3-P
NAD+
NADH
FadB
FadB
H_2O
Glyceraldehyde-3-phosphate dehydrogenase
NAD+
NADH
AcetylCoA
3-hydroxyacyl-CoA
1,3 -Biphosphoglycerate
Phosphoglycerate kinase
ADP
ATP
Krebs cycle
3-ketothiolase
3-Phosphoglycerate
CoASH
Butyryl-CoA
Phosphoglycerate mutase
3-ketothiolase
FadB
FAD
$FADH_2$
2-Phosphoglycerate
Acetoacetyl-CoA
Butenoyl-CoA
Enolase
ATP
AMP
Acetoaceyl-CoA synthetase
PhaJ
H_2O
Phosphoenolpyruvate
Pyruvate kinase
ADP
ATP
Acetoacetic acid
S(3)-Hydroxybutyryl-CoA
Pyruvate
R (3) – hydroxybutyrate dehydrogenase
Acetoacetyl-CoA reductase
NAD+
NADH
CoASH
NAD+
NADH
CO_2
Pyruvate dehydrogenase
R (3)-hydroxybutyrate
Epimerase
Acetyl-CoA
CoASH
3 x C
Depolymerase
NADPH
NADP+
Synthase
P3(HB)
R(3)-Hydroxybutyryl-CoA
Acetoacetyl-CoA reductase
β-Kethothiolase
Acetoacetyl-CoA
C12
CoASH
NAD+ NADH

Figure 2

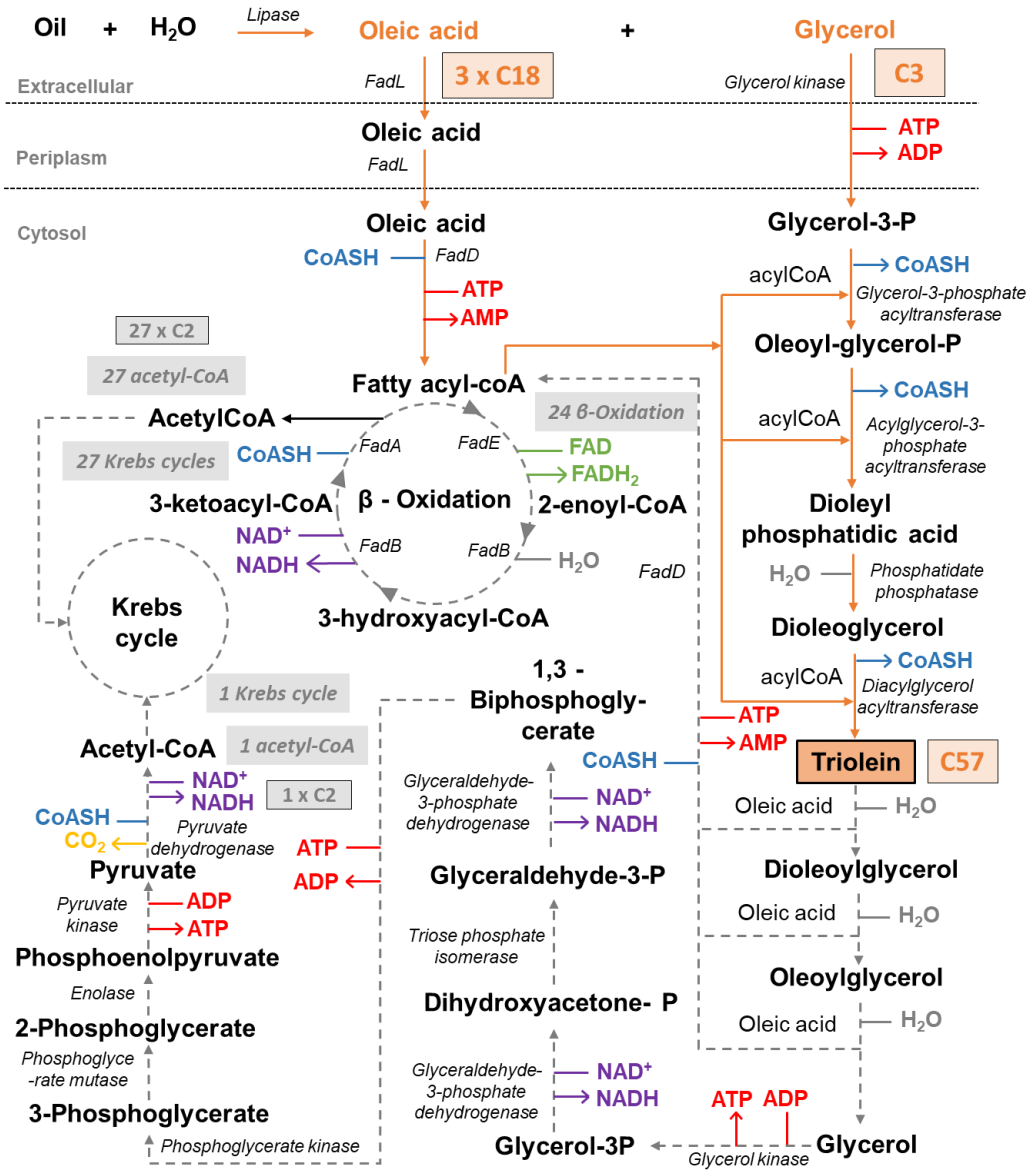
Oil + H2O
Lipase
Oleic acid + Glycerol
Extracellular
FadL
3 x C18
Glycerol kinase
C3
Periplasm
Oleic acid
ATP
ADP
FadL
Cytosol
Oleic acid
Glycerol-3-P
CoASH
FadD
ATP
AMP
acylCoA
CoASH
Glycerol-3-phosphate acyltransferase
Oleoyl-glycerol-P
27 x C2
27 acetyl-CoA
Fatty acyl-coA
24 ß-Oxidation
AcetylCoA
acylCoA
CoASH
27 Krebs cycles
CoASH
FadA
FadE
FAD
FADH2
Acylglycerol-3-phosphate acyltransferase
3-ketoacyl-CoA
β - Oxidation
2-enoyl-CoA
Dioleyl phosphatidic acid
NAD+
NADH
FadB
FadB
H2O
FadD
H2O
Phosphatidate phosphatase
Krebs cycle
3-hydroxyacyl-CoA
Dioleoglycerol
1,3 - Biphosphogly-cerate
acylCoA
CoASH
Diacylglycerol acyltransferase
1 Krebs cycle
ATP
AMP
Triolein
C57
Acetyl-CoA
1 acetyl-CoA
CoASH
Glyceraldehyde-3-phosphate dehydrogenase
NAD+
NADH
Oleic acid
H2O
NAD+
NADH
1 x C2
CoASH
CO2
Pyruvate dehydrogenase
ATP
ADP
Pyruvate
Glyceraldehyde-3-P
Dioleoylglycerol
Pyruvate kinase
ADP
ATP
Oleic acid
H2O
Triose phosphate isomerase
Phosphoenolpyruvate
Oleoylglycerol
Enolase
Dihydroxyacetone- P
Oleic acid
H2O
2-Phosphoglycerate
Glyceraldehyde-3-phosphate dehydrogenase
NAD+
NADH
ATP
ADP
Phosphoglyce -rate mutase
3-Phosphoglycerate
Glycerol-3P
Glycerol kinase
Glycerol
Phosphoglycerate kinase

Figure 3

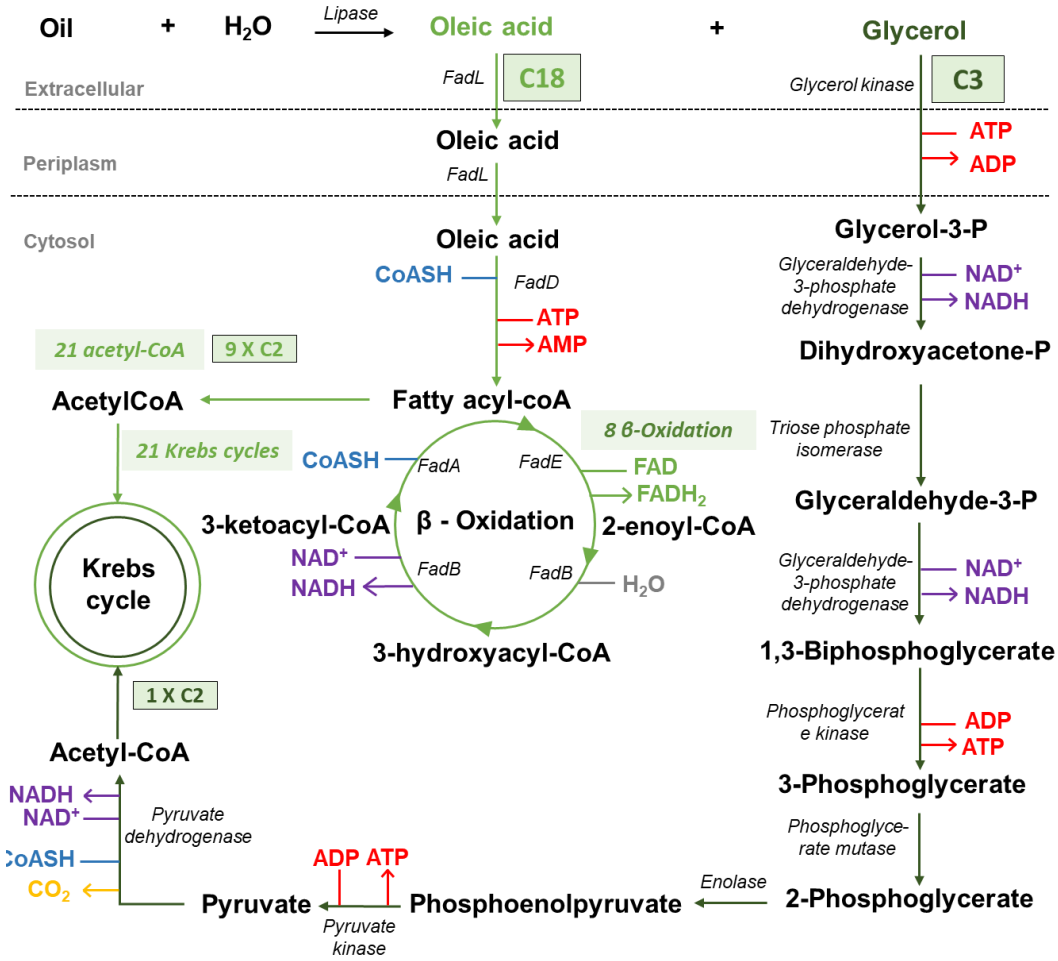
Oil
+
H2O
Lipase
Oleic acid
+
Glycerol
Extracellular
FadL
C18
Glycerol kinase
C3
Periplasm
Oleic acid
FadL
ATP
ADP
Cytosol
Oleic acid
Glycerol-3-P
CoASH
FadD
Glyceraldehyde-3-phosphate dehydrogenase
NAD+
NADH
ATP
AMP
21 acetyl-CoA
9 X C2
Dihydroxyacetone-P
AcetylCoA
Fatty acyl-coA
8 ß-Oxidation
Triose phosphate isomerase
21 Krebs cycles
CoASH
FadA
FadE
FAD
FADH2
Glyceraldehyde-3-P
3-ketoacyl-CoA
β - Oxidation
2-enoyl-CoA
Krebs cycle
NAD+
NADH
FadB
FadB
H2O
Glyceraldehyde-3-phosphate dehydrogenase
NAD+
NADH
3-hydroxyacyl-CoA
1,3-Biphosphoglycerate
1 X C2
Phosphoglycerate kinase
ADP
ATP
Acetyl-CoA
3-Phosphoglycerate
NADH
NAD+
Pyruvate dehydrogenase
Phosphoglycerate mutase
CoASH
CO2
ADP ATP
Enolase
Pyruvate
Phosphoenolpyruvate
2-Phosphoglycerate
Pyruvate kinase

Figure 4

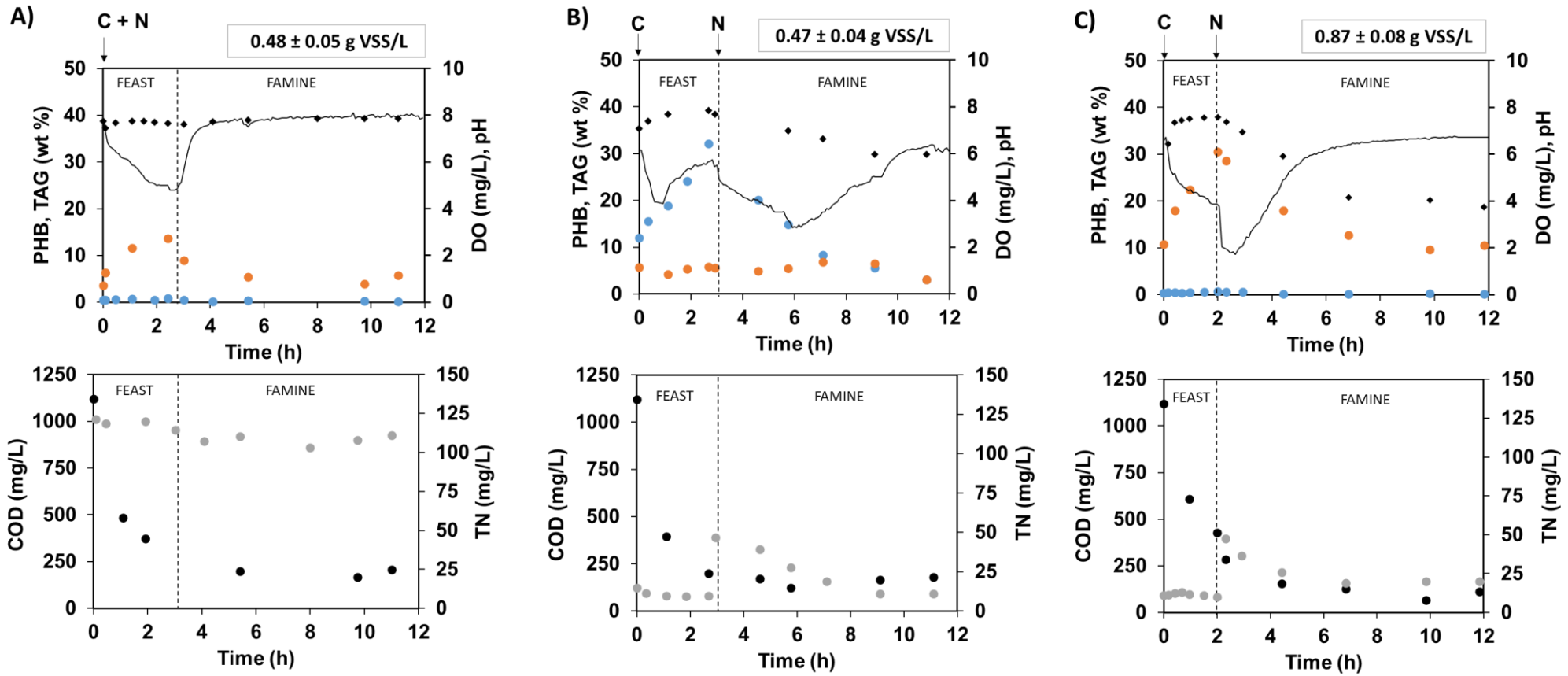
A)
C + N
0.48 ± 0.05 g VSS/L
FEAST
FAMINE
PHB, TAG (wt %)
DO (mg/L), pH
Time (h)
COD (mg/L)
TN (mg/L)
B)
C
N
0.47 ± 0.04 g VSS/L
C)
0.87 ± 0.08 g VSS/L

Figure 5

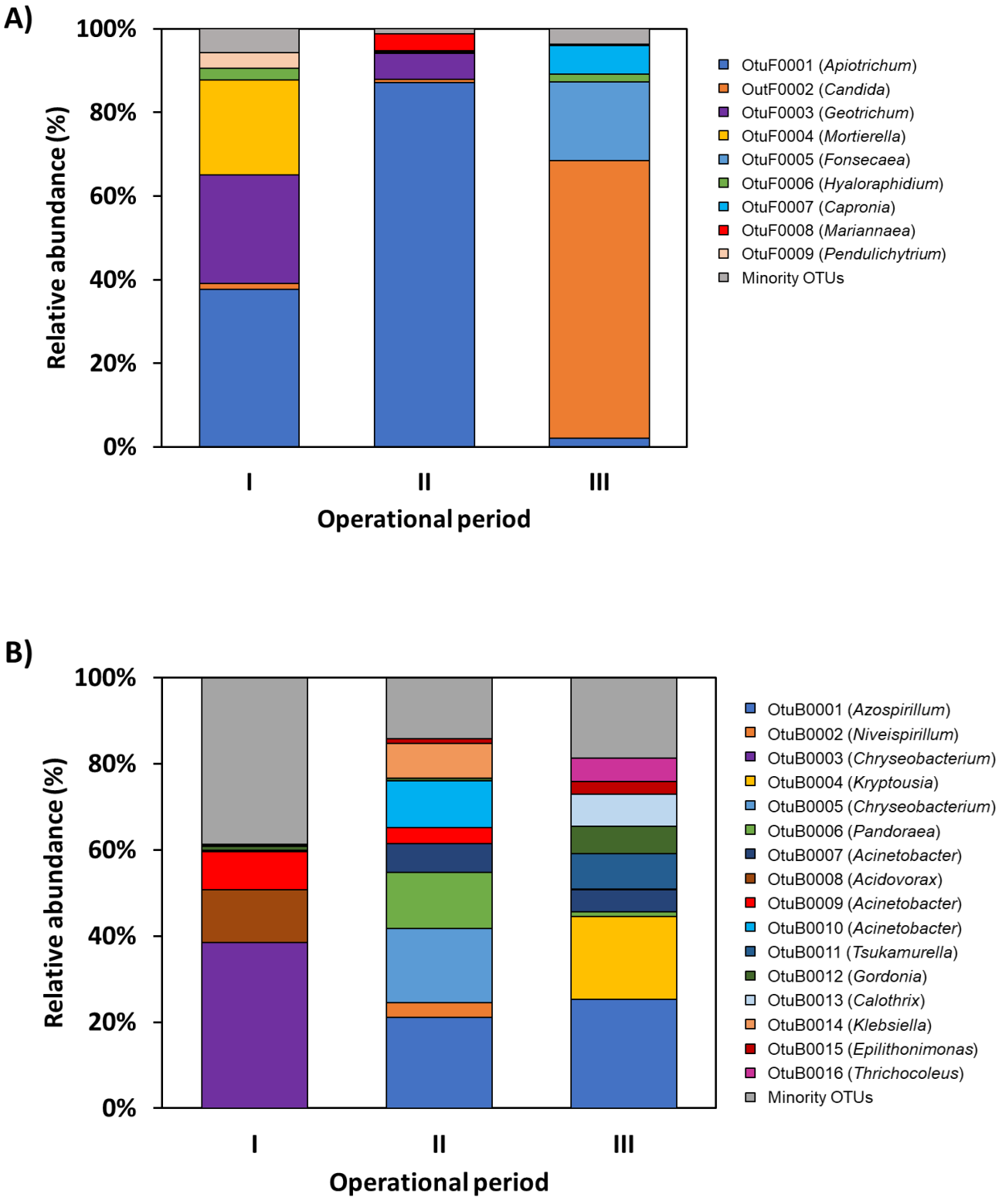
A)
100%
80%
60%
40%
20%
0%
Relative abundance (%)
I
II
III
Operational period
OtuF0001 (Apiotrichum)
OutF0002 (Candida)
OtuF0003 (Geotrichum)
OtuF0004 (Mortierella)
OtuF0005 (Fonsecaea)
OtuF0006 (Hyaloraphidium)
OtuF0007 (Capronia)
OtuF0008 (Mariannaea)
OtuF0009 (Pendulichytrium)
Minority OTUs
B)
100%
80%
60%
40%
20%
0%
Relative abundance (%)
I
II
III
Operational period
OtuB0001 (Azospirillum)
OtuB0002 (Niveispirillum)
OtuB0003 (Chryseobacterium)
OtuB0004 (Kryptousia)
OtuB0005 (Chryseobacterium)
OtuB0006 (Pandoraea)
OtuB0007 (Acinetobacter)
OtuB0008 (Acidovorax)
OtuB0009 (Acinetobacter)
OtuB0010 (Acinetobacter)
OtuB0011 (Tsukamurella)
OtuB0012 (Gordonia)
OtuB0013 (Calothrix)
OtuB0014 (Klebsiella)
OtuB0015 (Epilithonimonas)
OtuB0016 (Thrichocoleus)
Minority OTUs

Valorization of lipid-rich wastewaters: a theoretical analysis to tackle the competition between polyhydroxyalkanoate and triacylglyceride-storing populations

Lucía Argiz [a]*, David Correa-Galeote [b], Ángeles Val del Río [a], Anuska Mosquera-Corral [a], Rebeca González-Cabaleiro [c]

[a] CRETUS Institute, Department of Chemical Engineering, Universidade de Santiago de Compostela, 15782 Santiago de Compostela, Galicia, Spain

[b] Department of Microbiology and Institute of Water Research, Universidad de Granada, Granada, Spain

[c] Department of Biotechnology, Delft University of Technology, Van der Maasweg 9, 2629 HZ Delft, The Netherlands

* Corresponding author: luciaargiz.montes@usc.es

1. EXPERIMENTAL PROCEDURE

Table S1. Characteristics and composition of the waste fish oil used as a substrate.

Parameter	Unit	Average value ± Standard deviation
pH		3.75 ± 0.20
Conductivity	(µS/cm)	0.60 ± 0.10
Density	(g/L)	900 ± 10
TS	(g/g)	0.853 ± 0.018
VS	(g/g)	0.852 ± 0.019
Nitrogen	(g/g)	0.00 ± 0.00
COD	(g/g)	2.50 ± 0.11
Lipids	(g/g)	0.826 ± 0.089
Composition [1]		
	C14:0 (Myristic)	0.06
	C14:1 (Myristoleic)	< 0.01
	C15:0 (Pentadecanoic)	< 0.01
	C16:0 (Palmitic)	8.78
	C16:1 (Palmitoleic, n-7)	0.66
	C17:0 (Heptadecanoic)	0.08
	C17:1 (Margaroleic)	0.10
	C18:0 (Stearic)	2.77
	C18:2 (Oleic, n-9+n-7)	64.84
	C20:0 (Linoleic, n-6)	13.21
	C18:3 (α-linoleic acid)	0.52
	C20:1 (Linoleic, n-3)	<0.01
	C18:4 (Eicosenoic, n-9)	0.35
	C20:4 (Arachidonic, n-6)	0.27
	C20:4(Eicosatetraenoic)	< 0.01
	C21:5 (Eicosapentaenoic, n-3, EPA)	< 0.01
	C21:5 (Heneicosapentaenoic, n-3)	0.05
	C22:5 (Docosapentaenoic, n-6)	< 0.01
	C22:5 (Docosapentaenoic, n-3, DPA)	< 0.01
	C22:6 (Docosahexaenoic, n-3, DHA)	0.18
	Others	< 0.01

[1] Results expressed in % of each fatty acid respect the total.
COD (chemical oxygen demand), TS (total solids), VS (volatile solids)

Table S2. Dilution water composition.

Compound	Unit	Value
K_2PO_4	(mg/L)	700
$MgSO_4$	(mg/L)	140
KCl	(mg/L)	100
KH_2PO_4	(mg/L)	650 - 1000
Allylthiourea	(mg/L)	2.5
Trace element solution [1]	(mL/L)	2.0

[1] See reference (Vishniac and Santer, 1957).

Table S3. Analytical methods and calculations.

Analytical methods	
DO, T	Portable multimeter Hq40D, Hach-Lange, USA
pH	pH and ion meter GLP 22, Crison, Spain
Conductivity	Portable conductivity meter Probe Sension + EC5 HACH, Spain
TS, VS, TSS, VSS	APHA/AWWA/WEF (2017)
COD	APHA/AWWA/WE (2017)
Lipids	APHA/AWWA/WEF (2017) Soxhlet extractor Jp Selecta 8001800, Spain
TN, TOC, TC, IC	TOC-L analyzer with the TNM-module, TOC-5000 Shimadzu, Japan
Storage compounds quantification	Smolders et al. (1994)
Fatty acids composition	Gas chromatography, ISO 12966-2:2011 (4.2) fast method and ISO 12966-4:2015
TAGs and PHAs composition	Gas chromatography, HP innovax column equipped with a FID, Agilent USA
Calculations [(1)]	
Active biomass (g)	$X = g\ VSS - (g\ TAG + g\ PHA)$
Intracellular TAGs, PHAs (wt %)	$TAG = g\ TAG / g\ VSS \cdot 100$ $PHA = g\ PHA / g\ VSS \cdot 100$
Maximum specific conversion rates (Cmmol/Cmmol·h)	$q_{TAG} = (Cmmol_{TAG} \cdot / h) / Cmmol_X$ $q_{PHA} = (Cmmol_{PHA} \cdot / h) / Cmmol_X$ $- q_{TAG} = (- Cmmol_{TAG} \cdot / h) / Cmmol_X$ $- q_{PHA} = (- Cmmol_{PHA} \cdot / h) / Cmmol_X$ $q_X = (Cmmol_X \cdot / h) / Cmmol_{oil}$
Production yields (Cmmol/Cmmol)	$Y_{TAG} = Cmmol_{TAG} / Cmmol_{oil}$ $Y_{PHA} = Cmmol_{PHA} / Cmmol_{oil}$ $Y_X = Cmmol_X / Cmmol_{oil}$

(1) See reference (Argiz et al., 2020).

Chemical oxygen demand (COD), dissolved oxygen (DO), flame injection detector (FID), inorganic carbon (IC), polyhydroxyalkanoates (PHAs), maximum specific conversion rate (q), triacylglycerides (TAGs), total carbon (TC), total nitrogen (TN), total organic carbon (TOC), total solids (TS), total suspended solids (TSS), volatile solids (VS), volatile suspended solids (VSS), active biomass (X), production yield (Y).

2. METABOLIC PATHWAYS ANALYSIS

The metabolic pathways for oleic acid and glicerol were constructed according to information found in the literature. They are described in Figures 1, 2, and 3 of the main article.

2.1 Substrate hydrolysis, transport, and activation

The fed oil is hydrolysed before subsequent metabolization. Hydrolysis is performed by extracellular lipases, lipolytic and hydrolytic enzymes that act on the carboxyl ester bonds in acylglycerols yielding long-chain fatty acids (LCFAs), and glycerol. Free LCFAs, in this specific case, oleic acid units, are then transported into the cell and converted into long-chain fatty acyl-CoA (oleoyl-CoA) esters (Becker, 2010; Jimenez-diaz et al., 2019; Shon et al., 2002) that can be stored as reserve materials (PHAs or TAGs) (Garay et al., 2014) and/or catabolized (direct respiration).

2.2 PHAs synthesis and degradation

P3(HB) synthesis

Oleic acid is primarily converted via the β-oxidation pathway into S(3)-hydroxybutyryl-CoA (Figure 1), compound that is epimerized into the R isomer (R (3)-hydroxybutyryl-CoA), which is finally polymerized to form intracellular P3(HB) (Jimenez-diaz et al., 2019; Koller et al., 2010; Numata et al., 2013; Taguchi, 2017; Tan et al., 2014). For P3(HB) synthesis, 3 moles of oleic acid are required. Each mole needs 7 complete β-oxidation rounds to yield one mole of butyryl-CoA, concomitantly producing 7 moles of acetyl-CoA.

The length of P3(HB) storage pathway was calculated by counting the reactions involved in the synthesis of one mole of P3(HB) from three moles of oleic acid (steps are indicated in brackets): hydrolysis [3], transport [6], activation [6], oleoyl-CoA β-oxidation into 21 acetyl-CoA [87], butyryl-CoA oxidation [3], butenoyl-CoA hydration [3], epimerization [3],HB synthesis [3], polymerization for P3(HB) synthesis [2]. In total, 116 steps are calculated.

The bioenergetics calculations for specific reactions of the intracellular P3(HB) synthesis, were performed using eq.1 assuming a temperature (T) of 25 ˚C and a pH of 7. The values for the standard energy of formation ($\Delta G'^0$) of the different metabolites were obtained from eQuilibrator-API (Noor et al., 2013). R is the universal gas constant, S the reactants, P de products and α and β the number of molecules of products and reactants, respectively.

$$\Delta G = \Delta G'^0 + R \cdot T \cdot \ln \frac{\sum P^{\alpha}}{\sum S^{\beta}} \qquad \text{(eq.1)}$$

The concentrations of conserved moieties (e.g. NADH, Coenzyme A, etc.) were obtained from Bennett et al. (2009). For other metabolites concentrations of 1 mM were assumed (Noor et al., 2014).

S(3)Hydroxybutyryl-CoA β-Oxidation

S(3)Hydroxybutyryl-CoA + NAD^+ ⟶ Acetoacetyl-CoA + NADH (r1)

$\Delta G'$ = 6.03 kJ/mol

S(3)Hydroxybutyryl-CoA to P3(HB) synthesis

S(3)Hydroxybutyryl-CoA ⟶ R(3)Hydroxybutyryl-CoA (r2)

$\Delta G'$ = - 0.4 kJ/mol

The net yield of ATP produced with the synthesis of P3(HB) was determined as a combination of the ATP produced via substrate-level phosphorylation (9) and the ATP yielded as a consequence of $FADH_2$ (1.5 mol ATP/mol FADH) and NADH (2.5 mol ATP/mol NADH) oxidation in the electron transport chain (Shestov et al., 2013). During P3(HB) synthesis 6 ATP are consumed for activation of oleic acid but 21 FADH (31.5 ATP) and 24 NADH (60 ATP) are produced. This implies a total of 85.5 moles of ATP produced per mole of P3(HB) synthetised.

O_2 consumption is estimated by calculating the moles of $FADH_2$ and NADH produced. If 21 $FADH_2$ and 24 NADH are generated in the P3(HB) synthesis, 90 electrons are released and hence a total of 22.5 mole of O_2 have to be reduced per mole of P3(HB).

Results are expressed per mole of carbon. In this case, the values obtained (116 steps, 108 moles of ATP and 67.5 moles of O_2) were divided by the moles of carbon contained in one

mole of oleic acid (54 Cmol). Therefore P3(HB) synthesis involves 2.15 steps/Cmol, 1.58 ATP/Cmol and 0.42 mole O_2/Cmol (Figure 1). (Calculations concerning steps, ATP and O_2 calculations are detailed in the xls file "*Oleic acid metabolism calculations"*).

A second precursor of P3(HB) synthesis is glycerol (Chatzifragkou and Papanikolaou, 2012). Three glycerol units can be phosphorylated to form glycerol-3-P to be converted into dihydroxyacetone phosphate, an intermediate of the glycolytic pathway that can be directed towards HB synthesis (Figure 1). This process requires 38 steps, 10.50 moles of ATP, and 1.5 moles of O_2. Dividing these values by 9 Cmoles contained in three moles of glycerol, P3(HB) synthesis from glycerol involves 4.22 steps/Cmol, 1.17 ATP/Cmol and 0.17 mol O_2/Cmol.

The β-oxidation generates acetyl-CoA, which can be considered as a second precursor for the synthesis of R(3)-hydroxybutyryl-CoA (Numata et al., 2013). This process requires 35 steps, produces 14.50 ATP, and needs 4.5 moles of O_2. Dividing these results by the 12 Cmoles needed for P3(HB) synthesis from oleic acid via acetyl-CoA, 2.92 steps/Cmol, 1.21 ATP/Cmol and 0.38 mole O_2/Cmol are involved. However, P3(HB) synthesis from acetyl-CoA thermodynamically difficult (r3) in comparison with acetyl-CoA oxidation in the TCA cycle (r4). Consequently, here it was assumed that P3(HB) synthesis occurred via hydroxyacyl-CoA.

Acetyl-CoA to P3(HB) synthesis

$$2\ \text{Acetyl-CoA} \longrightarrow \text{Acetoacetyl-CoA} + \text{CoASH} \qquad \text{(r3)}$$

$\Delta G' = -12.15$ kJ/mol

Acetyl-CoA oxidation in the TCA cycle

$$\text{Oxaloacetate} + \text{Acetyl-CoA} + H_2O \longrightarrow \text{Citrate} + \text{CoASH} \qquad \text{(r4)}$$

$\Delta G' = 41.93$ kJ/mol

P3(HB) degradation

Intracellular PHB granules degradation involve P3(HB) depolymerization (Jimenez-diaz et al., 2019). Each R(3)-hydroxybutyrate unit is oxidized into acetoacetic acid, which is converted into acetoacetyl-CoA to be subsequent transformed into two acetyl-CoA that enter the TCA

Cycle (Kawaguchi and Doi, 1992). Calculations were performed according to previous section. In total, P3(HB) (12 Cmoles) mobilization involved 71 steps, 20.50 ATP and 4.50 moles of O_2,.That is to say, 5.92 steps/Cmol, 5.13 ATP/Cmol, and 1.13 mole O_2/Cmol (Figure 1).

2.3 TAGs storage and degradation

Triolein synthesis

In our experimental system, TAG is assumed to be composed of three units of oleic acid and one of glycerol released during substrate hydrolysis (Alvarez, 2016; Amara et al., 2016; Kumar et al., 2020; Thomson et al., 2010; Xia et al., 2014). TAG is synthetised via the ex *novo* pathway, the dominant pathway followed by yeasts in presence of high concentrations of hydrophobic compounds (Magdouli et al., 2014; Patel and Matsakas, 2019). This biotransformation is a growth-associated process that occurs simultaneously with the production of lipid-free material independent of the nitrogen exhaustion in the medium (Papanikolaou and Aggelis, 2010; Vasiliadou et al., 2018).

Firstly, glycerol-3-P inside the cell is acylated to form oleoyl-glycerone-P, which is further condensed with another acyl-CoA to produce dioleoyl phosphatidic acid. Then, it is dephosphorylated to produce dioleoglycerol and finally, a third acyl-CoA is incorporated leading to the formation of triolein (Alvarez and Steinbüchel, 2003; Liang and Jiang, 2013) (Figure 2). In this case, it was assumed that lipids stored via ex *novo* pathway presented a similar fatty acid composition to that of the substrate. However, intracellular compounds might participate in further endogenous biotransformations leading to compositional changes commonly upgrading the fatty acids profile (Aggelis et al., 1995; Carsanba et al., 2018; Patel and Matsakas, 2019).

Pathway's length, ATP yield, and oxygen consumption regarding triolein storage (20 steps, - 7 ATP and 0 moles of O_2) were calculated as explained in section *P3(HB) synthesis*. Results consider that 57 Cmole are needed for TAG synthesis (54 concerning three oleic acid units

and 3 one glycerol) (Figure 2). Therefore, triolein storage involves 0.35 steps/Cmol, - 0.12 ATP/Cmol, and does not require oxygen.

Triolein degradation

Regarding mobilization, triolein is first intracellularly hydrolyzed yielding three oleoyl-CoA units and one glycerol (Kulminskaya and Oberer, 2020). Then, the oleoyl-CoAs enter the β-oxidation pathway yielding 27 acetyl-CoAs per three moles of oleoyl-CoAs. These are finally degraded in the TCA cycle (Amara et al., 2016; Carsanba et al., 2018; Patel and Matsakas, 2019). Glycerol oxidation starts with its phosphorylation to produce glycerol-3-P. It is then converted into dihydroxyacetone phosphate, which is transformed into pyruvate finally yielding one acetyl-CoA that enters the TCA.

Triolein mobilization requires 398 steps, produces 360 moles of ATP, and consumes 81.5 moles of O_2. Considering that TAG contains 57 Cmoles, 6.98 steps/Cmol, 6.64 ATP/Cmol and 1.43 mole O_2/Cmol are involved (Figure 2).

2.4 Direct respiration

Oleoyl-CoA respiration requires the repetition of a sequence of reactions (β-oxidation) that result in the removal of two carbon atoms per round bringing acetyl-CoA at the end of the cycles. In the case of oleic acid, 8 β-oxidation rounds are needed for complete oleoyl-CoA oxidation yielding 9 acetyl-CoA that enter in the TCA (9 rounds) generating energy through the respiratory chain (Figure 3) (Becker, 2010; Shon et al., 2002). The respiration of one mole of oleic acid requires 128 steps, produces 120 moles of ATP, and consumes 26 moles of O_2. Therefore, this process involves 7.11 steps/Cmol, 6.67 ATP/Cmol, and 1.44 mole O_2/Cmol.

Glycerol might be also directly used for respiration (same pathway as the one considered in section *Triolein degradation*). In this case, per mole of glycerol (3 Cmoles) 19 steps are need, 16 moles of ATP are produced and 1.5 moles of O_2 are consumed (6.33 steps/Cmol, 5.22 ATP/Cmol, and 0.50 mole O_2/Cmol).

3. MICROBIAL ANALYSIS

The different operational strategies implemented in the SBR lead to important changes in the composition of the dominant fungal and bacterial genera present within the community. These variations correlate with the experimentally observed degree of substrate hydrolysis, and preferent storage compound accumulated throughout periods I – III.

3.1 Fungal community

When C and N feedings were uncoupled adding the C source in excess but at a similar rate as oxygen, and nitrogen (limited) three hours later (Period II, Figure 4.B); genus *Geotrichum* (OtuF0003) and *Mortierella* (OtuF0004) decreased their RAs from 26.0 % and 22.8 %, to 6.21 % and 0.33 % respectively, whereas *Apiotrichum* (OtuF0001) increased its RA from 37.8 % to 87.2 % (Figure 5.A) in comparison with when an excess of C and N were fed together at the beginning of the cycle (Period I, Figure 4.A). This correlates with the experimentally observed lower degree of hydrolysis and the decrease in TAG storage between periods I and II (Figure 4.A, 4.B). Thus, *Geotrichum* (OtuF0003) has been reported to be cultivated on hydrophobic substrates being capable of secreting extracellular lipases (Hlavsová et al., 2009) and assimilating carbon sources such as fats and oils to use them for growth and storage (Papanikolaou et al., 2017; Patel et al., 2019). The same occurs with *Mortierella* (OtuF0004), although it has been widely used for single-cell oils production using different sugars as carbon source (Athenaki et al., 2018; Demir and Gündes, 2020; Papanikolaou et al., 2004; Patel et al., 2020), this mould was also reported to be able to secrete lipases (Jermsuntiea et al., 2011; Kotogán et al., 2018) and produce lipids from hydrophobic substrates such as triolein or sesame oil (Papanikolaou and Aggelis, 2019). However, regarding *Apiotrichum* (OtuF0001), although it is a well-known oleaginous yeast, it has been only identified as capable of growing and storing lipids on hydrophilic substrates such as whey permeate (Ykema et al., 1989), tomato juice (Akindumila and Glatz, 1998), glucose (Papanikolaou and Aggelis, 2011), volatile fatty acids (VFAs) (Qian et al., 2021), or binary mixtures of free long-chain fatty acids (Lee et al., 1993). To the best of the author's knowledge, it has not been reported as a lipase producer.

After moving forward one hour N addition maintaining C and N feedings uncoupled (higher carbon excess during the feast phase) (Period III, Figure 4.C), *Apiotrichum's* (OtuF0001) RA decreased from 88.2 % to 2.1 %, being the main fungal genus *Candida* (OtuF0002) (66.4 %), followed by *Fonsecaea* (OtuF0005) (18.7 %) and *Capronia* (6.9 %) (Figure 5.A). These important variations match with the experimentally observed increase in the degree of substrate hydrolysis, and the shift in the preferent storage compound accumulated from PHA to TAG between periods II and III (Figure 4.B, 4.C, respectively). Thus, oleaginous yeasts belonging to the genus *Candida* (OtuF0002) have been widely recorded to use not only hydrophilic, but also hydrophobic substrates (i.e. triolein, olive oil, linseed oil) via the *ex novo* pathway (Dias et al., 2021; Papanikolaou and Aggelis, 2011) and stand out by their ability to hydrolize lipids (Theerachat et al., 2017). In fact, their microbial lipases are considered highly valuable and present wide applicability in industries such as textile, biodiesel, or agri-food (Chandra et al., 2020). *Fonsecaea* (OtuF0005), it has not been identified as an oleaginous fungus although it was demonstrated its ability to produce high levels of secretory lipases (Okeke and Gugnani, 1989). Certain species belonging to genera *Capronia* (OTUF0007) were identified as capable of degrading lipids and exhibit strong lipase activity although there is no information concerning lipids storage (Untereiner and Malloch, 1999).

3.2 Bacterial community

During period I, *Chryseobacterium* (OtuB0003, OtuB0005) (38.5 %), *Acidovorax* (OtuB0008) (12.2 %) and *Acinetobacter* (OtuB0009) (9.0 %) were the main bacterial genera (Figure 5.B). However, after changing the feeding strategy between periods I (coupled C and N feedings) and II (C supply at the beginning of the cycle and N feeding after 3 hours), genera *Chryseobacterium* (Otu0003B, Otu0005B) reduced its abundance from 38.5 % to 17.2 % and *Acidovorax* (Otu0008B) virtually disappeared (RA < 1 %). However, *Acinetobacter* (Otu0007B, Otu0009B, Otu0010B) raised its RA from 9.0 % to 21.2 %, and genera *Azospirillum* (Otu0001), *Pandoraea* (OtuB0006) and *Klebsiella* (OtuB0014) went from being minority OTUs to present RAs of 21.06 %, 13.0 % and 8.2 %, respectively (Figure 5.B).

Changes in the bacterial community correlate with the increase and preferent PHA storage observed between periods I and II (Figure 4.A, 4.B). Those genera that notably raised their RAs after changing the feeding strategy were all identified as PHA storing populations. Bacteria belonging to genera *Azospirillum* have been reported as capable of storing high PHA from substrates like acetate, pyruvate, lactate, and malate (Alves et al., 2017; Cassán et al., 2015; Itzigsohn et al., 1995; Martínez-Martínez et al., 2019) Regarding *Pandoraea,* it was observed to accumulate PHA from waste frying oil (de Paula et al., 2017) and other industrial by-products like lignin derivatives (Kumar et al., 2017, 2018; Liu et al., 2019), sugar cane molasses, permeate cheese whey or crude glycerol (de Paula et al., 2017). Also, *Klebsiella* has been widely identified as a very promising PHA producer (Ferreira et al., 2016; Wong et al., 2002) due to the high production yields that can be obtained on low-cost substrates (Valdez-Calderón et al., 2020; Wong et al., 2002). Besides, *Klebsiella* species present an active lipase system that makes them capable to hydrolize and assimilate hydrophobic substrates such as waste frying oil (Tufail et al., 2017). Regarding *Acinetobacter*, several research works reported the high PHA synthetic yield from a wide variety of substrates (VFAs, glucose, glycerol, etc.) including cooking oils (Giraldo-Montoya et al., 2020; Li et al., 2020; Muangwong et al., 2016; Sabapathy et al., 2020) due to their ability to secrete lipolytic enzymes (Liu et al., 2013; Sharma et al., 2019). Nonetheless, *Acinetobacter* species are also capable of storing TAG from both hydrophilic (glucose, xylose, acetate, pyruvate, etc.) (Alvarez and Steinbüchel, 2003; Manilla-Pérez et al., 2010; Salcedo-Vite et al., 2019; Wältermann et al., 2005) and hydrophobic substrates including olive oil (Alvarez et al., 1997; Alvarez and Steinbüchel, 2003), which explains their presence when TAG were preferently stored. Regarding those bacteria that decreased their abundance, to the best of the author's knowledge, *Chryseobacterium* have not been found as storing populations while *Acidovorax* were identified in PHA production processes using enriched activated sludge but hydrophilic carbon sources derived from pretreated substrates (Pereira et al., 2020; Yin et al., 2020).

After moving forward one hour N addition maintaining C and N feedings uncoupled (period III), *Azospirillum* (Otu0001) abundance was almost maintained (21.1 % vs 25.3 %). However,

PHA-storing genera *Pandoraea* (OtuB0006), *Chryseobacterium* (Otu0003B, Otu0005B) and *Klebsiella* (OtuB0014) became minority OTUs (RAs < 0.5 %), and *Acinetobacter* (Otu0007B, Otu0009B, Otu0010B) diminished its RA from 21.2 % to 5.3 %. On the contrary, species belonging to genera *Kryptousia* (OtuB0004) (19.2 %), *Tuskamurella* (OtuB0011) (8.1 %), *Gordonia* (Otu0012) (6.4 %), *Calothrix* (Otu0013) (7.4 %) and *Trichocoleus* (OtuB0016) (5.4 %), became dominant (Figure 5.B).

These changes observed in the bacterial community composition also match with the sharp modification in the preferent storage compound accumulated from PHA (Figure 4.A) to TAG (Figure 4.B). On the one hand, PHA-storing genera (*Pandoraea* (OtuB0006), *Chryseobacterium* (Otu0003B, Otu0005B), *Klebsiella* (OtuB0014), and *Acinetobacter* (Otu0007B, Otu0009B, Otu0010B)) RAs notably decreased. On the other hand, those storing-populations that increased their abundances were TAG producers. Genera *Calothrix* was recently identified as capable of storing TAGs (Santana-Sánchez et al., 2021) and *Gordonia* was observed to produce TAGs from different agro-industrial wastes including hydrophobic plant oils (Gouda et al., 2008; Uludag-Demirer et al., 2019). The rest of microorganisms that raised their abundance (*Kryptorusia*, *Tsukamurella*, and *Thrichocoleus)* have not been identified so far as TAG or PHA accumulators although *Tsukamurella* was recently reported to be a lipase producer (Huang et al., 2016).

4. pH DECREASE IN THE FAMINE PHASE

After nitrogen addition (NH_4Cl) a reduction of the medium pH when both PHA and TAG were preferentially stored, was observed due to NH_3 consumption by the biomass (Figure 4.B and 4.C, respectively) (Yamanaka, 1999). Only when the nitrogen source was depleted, the pH of the medium stabilized (Figure 4.B, 4.C). Although $NaHCO_3$ was added at the beginning of the cycle (Figure 4.B, Figure 4.C), this only allowed for the maintenance of the buffering capacity during the feast phase. Theoretical charge balances calculated by Newton-Raphson method showed this effect. Considering the addition of 1.79 g oleic acid (pKa_1 = 9.85 (Salentinig et al., 2010)), 0.57 g NH_4Cl (pKa_1 = 9.24) and 0.75 g $NaHCO_3$ (pKa_1 = 6.32, pKa_2 = 10.32)) per cycle, the pH would decrease along with NH_4Cl consumption as showed in Figure S2.

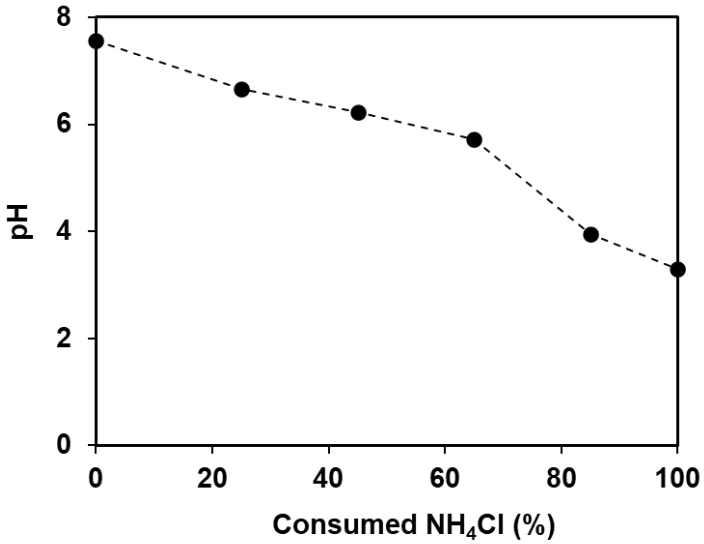

Figure S1. pH evolution along with NH_4Cl consumption in the reaction medium.

Nonetheless, in period III (Figure 4.C), the pH at the end of the cycle dropped to a lower value in comparison to period II (Figure 4.B). Given that oleic acid does not affect the medium pH and almost the same amount of NH_4Cl was consumed, only a lower $NaHCO_3$ supply to the reaction medium at the beginning of the feast phase could cause this sharper decrease in the pH during the famine phase. Although the same $NaHCO_3$ was weighted to prepare the dilution water in periods II and III, its presumable hydration led to a reduction of the IC.

5. SUBSTRATE HYDROLYSIS ESTIMATION

The degree of hydrolysis was estimated by the performance of COD balances between the beginning of the cycle and the end of the feast phase (maximum intracellular storage). The percentage of hydrolysis was calculated according to eq.10.

$$\%\, Hydrolysis = \frac{COD_{PHA} + COD_{TAG} + COD_S + COD_X}{COD_T} \quad \text{(eq.10)}$$

Where COD_T is the theoretical COD fed to the system, $COD_{PHA,}$ and COD_{TAG} the COD intracellularly accumulated during the feast phase, COD_S the non-consumed soluble COD_S measured at the end of the feast phase, and COD_X the COD used for growth during the feast phase.

Estimated hydrolysis percentages at the end of the feast phase for the cycles analyzed during periods I, II, and III were 45 %, 35 %, and 75 %, respectively. Figure SM2 shows two photographs of the non-hydrolysed substrate taken during period II.

Figure SM2. Non-hydrolyzed substrate in period II.

6. NITROGEN BALANCE

Experimental biomass productions in the famine phase during periods II (40 ± 5 mmol) and III (68 ± 10 mmol) were compared with the theoretical potential biomass productions. These were calculated assuming $CH_{1.75}O_{0.43}N_{0.22}$ (*Klebsiella*) and $CH_{1.66}O_{0.44}N_{0.12}$ (*Candida*) as the biomass formulas for the cultures enriched in PHA (period II) and TAG producers (period III) (Popovic, 2019) respectively, following the identified dominant genera in periods II and III (Figure 5).

Therefore, 0.22 and 0.12 mmoles of N are needed to produce one mmole of PHA and TAG-rich biomass. Given that in both cases 9 Nmmol were consumed during the famine phase, 39 and 71 mmol of biomass may be generated, respectively. Theoretical values match experimental results obtained.

7. C/O_2 RATIOS FOR PHA AND TAG SYNTHESIS

7.1 P3(HB) synthesis

According to the metabolic pathways, 0.42 mol O_2/Cmol are needed for P3(HB) synthesis via hydroxyacyl-CoA (Figure 1). This translates into 2.38 Cmol/mol O_2 (eq.2). Considering that one mole of P3(HB) contains 12 Cmoles and that 3 moles of oleic acid are needed for P3(HB) synthesis via hydroxyacyl-CoA, 0.60 moles of oleic acid per mole of O_2 are required for the storage of one mole of P3(HB) (eq. 3).

$$\frac{1}{\frac{0.42\ mol\ O_2}{Cmol\ P3(HB)\ stored}} = \frac{2.38\ Cmol\ P3(HB)\ stored}{mol\ O_2} \qquad \text{(eq.2)}$$

$$\frac{2.38\ Cmol\ P3(HB)\ stored}{mol\ O_2} \cdot \frac{1\ mol\ P3(HB)}{12\ Cmol} \cdot \frac{3\ mol\ oleic\ acid}{mol\ P3(HB)} = \frac{0.60\ mol\ oleic\ acid}{mol\ O_2} \qquad \text{(eq.3)}$$

7.2 Triolein synthesis

TAG synthesis needs 0.12 moles of ATP per Cmole to produce one mole of triolein (Figure 2). Thus, three oleic acid moles and one mole of glycerol are needed to be activated for its synthesis. Given that respiration is the only possible ATP source, and considering that oleic acid respiration yields 6.67 moles of ATP per Cmole, 0.018 Cmoles of oleic acid have to be oxidized to synthesize one mole of triolein (eq.4). Considering that respiration involves the consumption of 1.44 mol O_2/Cmol (Figure 3), to oxidize these 0.018 Cmoles of oleic acid, 0.026 moles of O_2 are required (eq.5). That is to say, 38.60 moles of triolein per mole of O_2 (eq.6). Therefore, if each mole of triolein contains 57 Cmoles and three moles of oleic acid, the moles of oleic acid (substrate) per mole of O_2 needed in triolein synthesis are 2.02 moles oleic acid per mole of O_2 (eq.7).

$$\overbrace{\frac{1\ Cmol}{6.67\ ATP}}^{\text{Direct respiration}} \cdot \overbrace{\frac{0.12\ ATP}{1\ Cmol}}^{\text{TAG storage}} = \frac{0.018\ Cmol\ oleic\ acid\ oxidized}{Cmol\ triolein\ stored} \qquad \text{(eq.4)}$$

$$\overbrace{\frac{1.44\ mol\ O_2}{Cmol} \cdot \frac{0.018\ Cmol\ oleic\ oxidized}{Cmol\ triolein\ stored}}^{\text{Direct respiration}} = \frac{0.026\ mol\ O_2}{Cmol\ triolein\ stored} \quad \text{(eq.5)}$$

$$\frac{1}{\frac{0.026\ mol\ O_2}{Cmol\ triolein\ stored}} = \frac{38.60\ Cmol\ triolein\ stored}{mol\ O_2} \quad \text{(eq.6)}$$

$$\frac{38.60\ Cmol\ triolein\ stored}{mol\ O_2} \cdot \frac{1\ mol\ triolein}{57\ Cmol} \cdot \frac{3\ mol\ oleic\ acid}{mol\ triolein} = \frac{2.02\ mol\ oleic\ acid}{mol\ O_2} \quad \text{(eq.7)}$$

7.3 Oleic acid respiration

As previously indicated, oleic acid respiration involves the consumption of 1.44 moles of O_2 per Cmole, this means 0.69 Cmoles oleic acid are consumed per mole O_2 (eq.8). Considering that one mole of oleic acid contains 18 Cmoles, 0.04 moles of oleic acid per mole of O_2 can be used for respiration (eq.9).

$$\frac{1}{\frac{1.44\ mol\ O_2}{Cmol\ oleic\ acid\ respirated}} = \frac{0.69\ Cmol\ oleic\ acid\ respirated}{mol\ O_2} \quad \text{(eq.8)}$$

$$\frac{0.69\ Cmol\ oleic\ acid\ respirated}{mol\ O_2} \cdot \frac{1\ mol\ oleic\ acid}{18\ Cmol} = \frac{0.04\ mol\ oleic\ acid}{mol\ O_2} \quad \text{(eq.9)}$$

The ratios of C/O_2 for each of the pathways are summarised in Table S4:

Table S4. C/O_2 influx ratios and oleic acid metabolization.

C/O_2 metabolic ratio	**Metabolic pathway**
0.60	P3(HB) accumulation
2.02	Triolein accumulation
0.04	Direct respiration

8. REFENCES

Aggelis, G., Komaitis, M., Papanikolaou, S., Papadopoulos, G., 1995. A mathematical model for the study of lipid accumulation in oleaginous microorganisms. I. Lipid accumulation during growth of Mucor circinelloides CBS 172-27 on a vegetable oil. Grasas y Aceites 46, 169–173. https://doi.org/10.3989/gya.1995.v46.i3.921

Akindumila, F., Glatz, B.A., 1998. Growth and oil production of Apiotrichum curvatum in tomato juice. J. Food Prot. 61, 1515–1517. https://doi.org/10.4315/0362-028X-61.11.1515

Alvarez, H.M., 2016. Triacylglycerol and wax ester-accumulating machinery in prokaryotes. Biochimie 120, 28–39. https://doi.org/10.1016/j.biochi.2015.08.016

Alvarez, H.M., Pucci, O.H., Steinbüchel, A., 1997. Lipid storage compounds in marine bacteria. Appl. Microbiol. Biotechnol. 47, 132–139. https://doi.org/10.1007/s002530050901

Alvarez, H.M., Steinbüchel, A., 2003. Triacylglycerols in prokaryotic microorganisms. Appl. Microbiol. Biotechnol. 60, 367–376. https://doi.org/10.1007/s00253-002-1135-0

Alves, L.P.S., Almeida, A.T., Cruz, L.M., Pedrosa, F.O., de Souza, E.M., Chubatsu, L.S., Müller-Santos, M., Valdameri, G., 2017. A simple and efficient method for poly-3-hydroxybutyrate quantification in diazotrophic bacteria within 5 minutes using flow cytometry. Brazilian J. Med. Biol. Res. 50, 1–10. https://doi.org/10.1590/1414-431X20165492

Amara, S., Seghezzi, N., Otani, H., Diaz-Salazar, C., Liu, J., Eltis, L.D., 2016. Characterization of key triacylglycerol biosynthesis processes in rhodococci. Sci. Rep. 6, 1–13. https://doi.org/10.1038/srep24985

Argiz, L., Fra-Vázquez, A., del Río, Á.V., Mosquera-Corral, A., 2020. Optimization of an enriched mixed culture to increase PHA accumulation using industrial saline complex wastewater as a substrate. Chemosphere 247. https://doi.org/10.1016/j.chemosphere.2020.125873

Athenaki, M., Gardeli, C., Diamantopoulou, P., Tchakouteu, S.S., Sarris, D., Philippoussis, A., Papanikolaou, S., 2018. Lipids from yeasts and fungi: physiology, production and analytical considerations. J. Appl. Microbiol. 124, 336–367. https://doi.org/10.1111/jam.13633

Becker, P., 2010. Understanding and Optimizing the Microbial Degradation of Olive Oil: A Case Study with the Thermophilic Bacterium Geobacillus thermoleovorans IHI-91, Olives

and Olive Oil in Health and Disease Prevention. Elsevier Inc. https://doi.org/10.1016/B978-0-12-374420-3.00042-5

Bennett, B.D., Kimball, E.H., Gao, M., Osterhout, R., Van Dien, S.J., Rabinowitz, J.D., 2009. Absolute metabolite concentrations and implied enzyme active site occupancy in Escherichia coli. Nat. Chem. Biol. 5, 593–599. https://doi.org/10.1038/nchembio.186

Carsanba, E., Papanikolaou, S., Erten, H., 2018. Production of oils and fats by oleaginous microorganisms with an emphasis given to the potential of the nonconventional yeast Yarrowia lipolytica. Crit. Rev. Biotechnol. 38, 1230–1243. https://doi.org/10.1080/07388551.2018.1472065

Cassán, F.D., Okon, Y., Creus, C.M., 2015. Handbook for *Azospirillum*.

Chandra, P., Enespa, Singh, R., Arora, P.K., 2020. Microbial lipases and their industrial applications: A comprehensive review, Microbial Cell Factories. BioMed Central. https://doi.org/10.1186/s12934-020-01428-8

Chatzifragkou, A., Papanikolaou, S., 2012. Effect of impurities in biodiesel-derived waste glycerol on the performance and feasibility of biotechnological processes. Appl. Microbiol. Biotechnol. 95, 13–27. https://doi.org/10.1007/s00253-012-4111-3

de Paula, F.C., Kakazu, S., de Paula, C.B.C., Gomez, J.G.C., Contiero, J., 2017. Polyhydroxyalkanoate production from crude glycerol by newly isolated Pandoraea sp. Polyhydroxyalkanoate production from crude glycerol. J. King Saud Univ. - Sci. 29, 166–173. https://doi.org/10.1016/j.jksus.2016.07.002

Demir, M., Gündes, A.G., 2020. Single-cell oil production by Mortierella isabellina DSM 1414 using different sugars as carbon source. Biotechnol. Prog. 36, 8–15. https://doi.org/10.1002/btpr.3050

Dias, K.B., Oliveira, N.M.L., Brasil, B.S.A.F., Vieira-Almeida, E.C., Paula-Elias, F.C., Almeida, A.F., 2021. Simultaneous High Nutritional Single Cell Oil and Lipase Production By Candida Viswanathii. Acta Sci. Pol. Technol. Aliment. 20, 93–102. https://doi.org/10.17306/J.AFS.0856

Ferreira, A.M., Queirós, D., Gagliano, M.C., Serafim, L.S., Rossetti, S., 2016. Polyhydroxyalkanoates-accumulating bacteria isolated from activated sludge acclimatized to hardwood sulphite spent liquor. Ann. Microbiol. 66, 833–842. https://doi.org/10.1007/s13213-015-1169-z

Garay, L.A., Boundy-Mills, K.L., German, J.B., 2014. Accumulation of high-value lipids in

single-cell microorganisms: A mechanistic approach and future perspectives. J. Agric. Food Chem. 62, 2709–2727. https://doi.org/10.1021/jf4042134

Giraldo-Montoya, J.M., Castaño-Villa, G.J., Rivera-Páez, F.A., 2020. Bacteria from industrial waste: potential producers of polyhydroxyalkanoates (PHAs) in Manizales, Colombia. Environ. Monit. Assess. 192. https://doi.org/10.1007/s10661-020-08461-5

Gouda, M.K., Omar, S.H., Aouad, L.M., 2008. Single cell oil production by Gordonia sp. DG using agro-industrial wastes. World J. Microbiol. Biotechnol. 24, 1703–1711. https://doi.org/10.1007/s11274-008-9664-z

Hlavsová, K., Zarevúcka, M., Wimmer, Z., Macková, M., Sovová, H., 2009. Geotrichum candidum 4013: Extracellular lipase versus cell-bound lipase from the single strain. J. Mol. Catal. B Enzym. 61, 188–193. https://doi.org/10.1016/j.molcatb.2009.06.012

Huang, J., Yan, R., He, J. yao, Wang, P., 2016. Purification and Immobilization of a Novel Enantioselective Lipase from Tsukamurella tyrosinosolvents for Efficient Resolution of Ethyl 2-(2-oxopyrrolidin-1-yl) Butyrate. Appl. Biochem. Biotechnol. 180, 609–622. https://doi.org/10.1007/s12010-016-2119-3

Itzigsohn, R., Yarden, O., Okon, Y., 1995. Polyhydroxyalkanoate analysis in Azospirillum brasilense. Can. J. Microbiol. 41, 73–76. https://doi.org/10.1139/m95-171

Jermsuntiea, W., Aki, T., Toyoura, R., Iwashita, K., Kawamoto, S., Ono, K., 2011. Purification and characterization of intracellular lipase from the polyunsaturated fatty acid-producing fungus Mortierella alliacea. N. Biotechnol. 28, 158–164. https://doi.org/10.1016/j.nbt.2010.09.007

Jimenez-diaz, L., Caballero, A., Segura, A., 2019. Aerobic Utilization of Hydrocarbons, Oils, and Lipids. Aerob. Util. Hydrocarb. Oils, Lipids 291–313. https://doi.org/10.1007/978-3-319-50418-6

Kawaguchi, Y., Doi, Y., 1992. Kinetics and Mechanism of Synthesis and Degradation of Poly(3-hydroxybutyrate) in Alcaligenes eutrophus. Macromolecules 25, 2324–2329. https://doi.org/10.1021/ma00035a007

Koller, M., Atlić, A., Dias, M., Reiterer, A., Braunegg, G., 2010. Industrial production of PHA from waste raw materials. Plast. from Bact. 14, 85–119. https://doi.org/10.1007/978-3-642-03287

Kotogán, A., Zambrano, C., Kecskeméti, A., Varga, M., Szekeres, A., Papp, T., Vágvölgyi, C., Takó, M., 2018. An organic solvent-tolerant lipase with both hydrolytic and synthetic

activities from the oleaginous fungus mortierella echinosphaera. Int. J. Mol. Sci. 19, 1–16. https://doi.org/10.3390/ijms19041129

Kulminskaya, N., Oberer, M., 2020. Protein-protein interactions regulate the activity of Adipose Triglyceride Lipase in intracellular lipolysis. Biochimie 169, 62–68. https://doi.org/10.1016/j.biochi.2019.08.004

Kumar, M., Rathour, R., Gupta, J., Pandey, A., Gnansounou, E., Thakur, I.S., 2020. Bacterial production of fatty acid and biodiesel: opportunity and challenges, Refining Biomass Residues for Sustainable Energy and Bioproducts. Elsevier Inc. https://doi.org/10.1016/b978-0-12-818996-2.00002-8

Kumar, M., Singhal, A., Verma, P.K., Thakur, I.S., 2017. Production and Characterization of Polyhydroxyalkanoate from Lignin Derivatives by Pandoraea sp. ISTKB. ACS Omega 2, 9156–9163. https://doi.org/10.1021/acsomega.7b01615

Kumar, Madan, Verma, S., Gazara, R.K., Kumar, Manish, Pandey, A., Verma, P.K., Thakur, I.S., 2018. Genomic and proteomic analysis of lignin degrading and polyhydroxyalkanoate accumulating β-proteobacterium Pandoraea sp. ISTKB. Biotechnol. Biofuels 11, 1–23. https://doi.org/10.1186/s13068-018-1148-2

Lee, I., Hammond, E.G., Cornette, J.L., Glatz, B.A., 1993. Triacylglycerol assembly from binary mixtures of fatty acids by Apiotrichum curvatum. Lipids 28, 1055–1061. https://doi.org/10.1007/BF02537070

Li, D., Yin, F., Ma, X., 2020. Towards biodegradable polyhydroxyalkanoate production from wood waste: Using volatile fatty acids as conversion medium. Bioresour. Technol. 299, 122629. https://doi.org/10.1016/j.biortech.2019.122629

Liang, M.H., Jiang, J.G., 2013. Advancing oleaginous microorganisms to produce lipid via metabolic engineering technology. Prog. Lipid Res. 52, 395–408. https://doi.org/10.1016/j.plipres.2013.05.002

Liu, C., Wang, H., Xing, W., Wei, L., 2013. Composition diversity and nutrition conditions for accumulation of polyhydroxyalkanoate (PHA) in a bacterial community from activated sludge. Appl. Microbiol. Biotechnol. 97, 9377–9387. https://doi.org/10.1007/s00253-013-5165-6

Liu, D., Yan, X., Si, M., Deng, X., Min, X., Shi, Y., Chai, L., 2019. Bioconversion of lignin into bioplastics by Pandoraea sp. B-6: molecular mechanism. Environ. Sci. Pollut. Res. 26, 2761–2770. https://doi.org/10.1007/s11356-018-3785-1

Magdouli, S., Yan, S., Tyagi, R.D., Surampalli, R.Y., 2014. Heterotrophic microorganisms: A promising source for biodiesel production. Crit. Rev. Environ. Sci. Technol. 44, 416–453. https://doi.org/10.1080/10643389.2012.728523

Manilla-Pérez, E., Lange, A.B., Hetzler, S., Steinbüchel, A., 2010. Occurrence, production, and export of lipophilic compounds by hydrocarbonoclastic marine bacteria and their potential use to produce bulk chemicals from hydrocarbons. Appl. Microbiol. Biotechnol. 86, 1693–1706. https://doi.org/10.1007/s00253-010-2515-5

Martínez-Martínez, M. de los A., González-Pedrajo, B., Dreyfus, G., Soto-Urzúa, L., Martínez-Morales, L.J., 2019. Phasin PhaP1 is involved in polyhydroxybutyrate granules morphology and in controlling early biopolymer accumulation in Azospirillum brasilense Sp7. AMB Express 9. https://doi.org/10.1186/s13568-019-0876-4

Muangwong, A., Boontip, T., Pachimsawat, J., Napathorn, S.C., 2016. Medium chain length polyhydroxyalkanoates consisting primarily of unsaturated 3-hydroxy-5-cis-dodecanoate synthesized by newly isolated bacteria using crude glycerol. Microb. Cell Fact. 15, 1–17. https://doi.org/10.1186/s12934-016-0454-2

Noor, E., Bar-Even, A., Flamholz, A., Reznik, E., Liebermeister, W., Milo, R., 2014. Pathway Thermodynamics Highlights Kinetic Obstacles in Central Metabolism. PLoS Comput. Biol. 10. https://doi.org/10.1371/journal.pcbi.1003483

Noor, E., Haraldsdóttir, H.S., Milo, R., Fleming, R.M.T., 2013. Consistent Estimation of Gibbs Energy Using Component Contributions. PLoS Comput. Biol. 9. https://doi.org/10.1371/journal.pcbi.1003098

Numata, K., Morisaki, K., Tomizawa, S., Ohtani, M., Demura, T., Miyazaki, M., Nogi, Y., Deguchi, S., Doi, Y., 2013. Synthesis of poly- and oligo(hydroxyalkanoate)s by deep-sea bacteria, Colwellia spp., Moritella spp., and Shewanella spp. Polym. J. 45, 1094–1100. https://doi.org/10.1038/pj.2013.25

Papanikolaou, S., Aggelis, G., 2019. Sources of microbial oils with emphasis to Mortierella (Umbelopsis) isabellina fungus. World J. Microbiol. Biotechnol. 35, 1–19. https://doi.org/10.1007/s11274-019-2631-z

Papanikolaou, S., Aggelis, G., 2011. Lipids of oleaginous yeasts. Part II: Technology and potential applications. Eur. J. Lipid Sci. Technol. 113, 1052–1073. https://doi.org/10.1002/ejlt.201100015

Papanikolaou, S., Aggelis, G., 2010. Yarrowia lipolytica: A model microorganism used for the production of tailor-made lipids. Eur. J. Lipid Sci. Technol. 112, 639–654.

https://doi.org/10.1002/ejlt.200900197

Papanikolaou, S., Komaitis, M., Aggelis, G., 2004. Single cell oil (SCO) production by Mortierella isabellina grown on high-sugar content media. Bioresour. Technol. 95, 287–291. https://doi.org/10.1016/j.biortech.2004.02.016

Papanikolaou, S., Rontou, M., Belka, A., Athenaki, M., Gardeli, C., Mallouchos, A., Kalantzi, O., Koutinas, A.A., Kookos, I.K., Zeng, A.P., Aggelis, G., 2017. Conversion of biodiesel-derived glycerol into biotechnological products of industrial significance by yeast and fungal strains. Eng. Life Sci. 17, 262–281. https://doi.org/10.1002/elsc.201500191

Patel, A., Karageorgou, D., Rova, E., Katapodis, P., Rova, U., Christakopoulos, P., Matsakas, L., 2020. An overview of potential oleaginous microorganisms and their role in biodiesel and omega-3 fatty acid-based industries. Microorganisms 8. https://doi.org/10.3390/microorganisms8030434

Patel, A., Matsakas, L., 2019. A comparative study on de novo and ex novo lipid fermentation by oleaginous yeast using glucose and sonicated waste cooking oil. Ultrason. Sonochem. 52, 364–374. https://doi.org/10.1016/j.ultsonch.2018.12.010

Patel, A., Pruthi, V., Pruthi, P.A., 2019. Innovative screening approach for the identification of triacylglycerol accumulating oleaginous strains. Renew. Energy 135, 936–944. https://doi.org/10.1016/j.renene.2018.12.078

Pereira, J., Queirós, D., Lemos, P.C., Rossetti, S., Serafim, L.S., 2020. Enrichment of a mixed microbial culture of PHA-storing microorganisms by using fermented hardwood spent sulfite liquor. N. Biotechnol. 56, 79–86. https://doi.org/10.1016/j.nbt.2019.12.003

Popovic, M., 2019. Thermodynamic properties of microorganisms: determination and analysis of enthalpy, entropy, and Gibbs free energy of biomass, cells and colonies of 32 microorganism species. Heliyon 5, e01950. https://doi.org/10.1016/j.heliyon.2019.e01950

Publishers, K.A., 1989. Lipases of Fonsecaea pedrosoi and Phialophora verrucosa Lipase production Lipase assay The lipase activity was estimated titrimetrically (Somkuti & Babel 1968). One 324, 313–324.

Qian, X., Zhou, X., Chen, L., Zhang, X., Xin, F., Dong, W., Zhang, W., Ochsenreither, K., Jiang, M., 2021. Bioconversion of volatile fatty acids into lipids by the oleaginous yeast Apiotrichum porosum DSM27194. Fuel 290, 119811. https://doi.org/10.1016/j.fuel.2020.119811

Sabapathy, P.C., Devaraj, S., Meixner, K., Anburajan, P., Kathirvel, P., Ravikumar, Y., Zabed, H.M., Qi, X., 2020. Recent developments in Polyhydroxyalkanoates (PHAs) production – A review. Bioresour. Technol. 123132. https://doi.org/10.1016/j.biortech.2020.123132

Salcedo-Vite, K., Sigala, J.C., Segura, D., Gosset, G., Martinez, A., 2019. Acinetobacter baylyi ADP1 growth performance and lipid accumulation on different carbon sources. Appl. Microbiol. Biotechnol. 103, 6217–6229. https://doi.org/10.1007/s00253-019-09910-z

Salentinig, S., Sagalowicz, L., Glatter, O., 2010. Self-assembled structures and pK a value of oleic acid in systems of biological levance. Langmuir 26, 11670–11679. https://doi.org/10.1021/la101012a

Santana-Sánchez, A., Lynch, F., Sirin, S., Allahverdiyeva, Y., 2021. Nordic cyanobacterial and algal lipids: Triacylglycerol accumulation, chemotaxonomy and bioindustrial potential . Physiol. Plant. 1–12. https://doi.org/10.1111/ppl.13443

Sharma, P.K., Mohanan, N., Sidhu, R., Levin, D.B., 2019. Colonization and degradation of polyhydroxyalkanoates by lipase-producing bacteria. Can. J. Microbiol. 65, 461–475. https://doi.org/10.1139/cjm-2019-0042

Shestov, A.A., Mancuso, A., Leeper, D.B., Glickson, J.D., 2013. Metabolic network analysis of DB1 melanoma cells: How much energy is derived from aerobic glycolysis? Adv. Exp. Med. Biol. 765, 265–271. https://doi.org/10.1007/978-1-4614-4989-8_37

Shon, H.K., Tian, D., Kwon, D.Y., Jin, C.S., Lee, T.J., Chung, W.J., 2002. Degradation of fat, oil, and grease (FOGs) by lipase-producing bacterium Pseudomonas sp. strain D2D3. J. Microbiol. Biotechnol. 12, 583–591.

Smolders, G.J.F., van der Meij, J., van Loosdrecht, M.C.M., Heijnen, J.J., 1994. Stoichiometric model of the aerobic metabolism of the biological phosphorus removal process. Biotechnol. Bioeng. 44, 837–848. https://doi.org/10.1002/bit.260440709

Taguchi, S., 2017. Bioengineering of Polyhydroxyalkanoates. Encycl. Polym. Sci. Technol. 1–9. https://doi.org/10.1002/0471440264.pst655

Tan, G.Y.A., Chen, C.L., Li, L., Ge, L., Wang, L., Razaad, I.M.N., Li, Y., Zhao, L., Mo, Y., Wang, J.Y., 2014. Start a research on biopolymer polyhydroxyalkanoate (PHA): A review. Polymers (Basel). 6, 706–754. https://doi.org/10.3390/polym6030706

Theerachat, M., Tanapong, P., Chulalaksananukul, W., 2017. The culture or co-culture of Candida rugosa and Yarrowia lipolytica strain rM-4A, or incubation with their crude extracellular lipase and laccase preparations, for the biodegradation of palm oil mill

wastewater. Int. Biodeterior. Biodegrad. 121, 11–18. https://doi.org/10.1016/j.ibiod.2017.03.002

Thomson, N., Summers, D., Sivaniah, E., 2010. Synthesis, properties and uses of bacterial storage lipid granules as naturally occurring nanoparticles. Soft Matter 6, 4045–4057. https://doi.org/10.1039/b927559b

Tufail, S., Munir, S., Jamil, N., 2017. Variation analysis of bacterial polyhydroxyalkanoates production using saturated and unsaturated hydrocarbons. Brazilian J. Microbiol. 48, 629–636. https://doi.org/10.1016/j.bjm.2017.02.008

Uludag-Demirer, S., Liao, W., Demirer, G.N., 2019. Volatile fatty acid production from anaerobic digestion of organic residues, Methods in Molecular Biology. https://doi.org/10.1007/978-1-4939-9484-7_20

Untereiner, W.A., Malloch, D., 1999. Patterns of substrate utilization in species of Capronia and allied black yeasts: Ecological and taxonomic implications. Mycologia 91, 417–427. https://doi.org/10.2307/3761342

Valdez-Calderón, A., Barraza-Salas, M., Quezada-Cruz, M., Islas-Ponce, M.A., Angeles-Padilla, A.F., Carrillo-Ibarra, S., Rodríguez, M., Rojas-Avelizapa, N.G., Garrido-Hernández, A., Rivas-Castillo, A.M., 2020. Production of polyhydroxybutyrate (PHB) by a novel Klebsiella pneumoniae strain using low-cost media from fruit peel residues. Biomass Convers. Biorefinery. https://doi.org/10.1007/s13399-020-01147-5

Vasiliadou, I.A., Bellou, S., Daskalaki, A., Tomaszewska-Hetman, L., Chatzikotoula, C., Kompoti, B., Papanikolaou, S., Vayenas, D., Pavlou, S., Aggelis, G., 2018. Biomodification of fats and oils and scenarios of adding value on renewable fatty materials through microbial fermentations: Modelling and trials with Yarrowia lipolytica. J. Clean. Prod. 200, 1111–1129. https://doi.org/10.1016/j.jclepro.2018.07.187

Vishniac, W., Santer, M., 1957. The *thiobacilli*. Bacteriol. Rev. 21, 195–213.

Wältermann, M., Hinz, A., Robenek, H., Troyer, D., Reichelt, R., Malkus, U., Galla, H.J., Kalscheuer, R., Stöveken, T., Von Landenberg, P., Steinbüchel, A., 2005. Mechanism of lipid-body formation in prokaryotes: How bacteria fatten up. Mol. Microbiol. 55, 750–763. https://doi.org/10.1111/j.1365-2958.2004.04441.x

White, D., Drummond, J., Fuqua, C., York, N., n.d. The Physiology and Biochemistry of Prokaryotes FOURTH EDITION.

Wong, P.A.L., Chua, H., Lo, W., Lawford, H.G., Yu, P.H., 2002. Production of specific

copolymers of polyhydroxyalkanoates from industrial waste. Appl. Biochem. Biotechnol. - Part A Enzym. Eng. Biotechnol. 98–100, 655–662. https://doi.org/10.1385/ABAB:98-100:1-9:655

Xia, E.H., Jiang, J.J., Huang, H., Zhang, L.P., Zhang, H. Bin, Gao, L.Z., 2014. Transcriptome analysis of the oil-rich tea plant, Camellia oleifera, reveals candidate genes related to lipid metabolism. PLoS One 9. https://doi.org/10.1371/journal.pone.0104150

Yamaguchi, T., Tsuchiya, T., Nakahara, S., Fukui, A., Nagamoto, Y., Murotani, K., Eshima, K., Takahashi, N., 2016. Efficacy of Left Atrial Voltage-Based Catheter Ablation of Persistent Atrial Fibrillation. J. Cardiovasc. Electrophysiol. 27, 1055–1063. https://doi.org/10.1111/jce.13019

Yamanaka, T., 1999. Utilization of inorganic and organic nitrogen in pure cultures by saprotrophic and ectomycorrhizal fungi producing sporophores on urea-treated forest floor. Mycol. Res. 103, 811–816. https://doi.org/10.1017/S0953756298007801

Yin, F., Li, D., Ma, X., Li, J., Qiu, Y., 2020. Poly(3-hydroxybutyrate-3-hydroxyvalerate) production from pretreated waste lignocellulosic hydrolysates and acetate co-substrate. Bioresour. Technol. 316, 123911. https://doi.org/10.1016/j.biortech.2020.123911

Ykema, A., Kater, M.M., Smit, H., 1989. Lipid production in wheypermeate by an unsaturated fatty acid mutant of the oleaginous yeast Apiotrichum curvatum. Biotechnol. Lett. 11, 477–482. https://doi.org/10.1007/BF01026645